EVALUATION AND VALIDATION OF SOFT ROBOTIC END EFFECTORS FOR PRODUCE HARVESTING

By

Zachary F. Dutcher

A THESIS

Submitted to
Michigan State University
in partial fulfillment of the requirements
for the degree of

Mechanical Engineering–Master of Science

2018

ABSTRACT

EVALUATION AND VALIDATION OF SOFT ROBOTIC END EFFECTORS FOR PRODUCE HARVESTING

By

Zachary F. Dutcher

Global population is expected to exceed 9 billion people by 2050 which will require a 70% increase in net global food production. 75% of global farm holdings are considered small at 2.5 acres or less. While contemporary industrial farming gains efficiency through increased mechanization, it comes with significant environmental costs. Industrial farming practices such as frequent tillage, monocropping and use of synthetic fertilizers, pesticides and herbicides are unsustainable practices that will continue to degrade the surrounding ecosystem. Small scale farms present an opportunity to utilize regenerative farming practices; however, they are potentially challenging to scale up and expensive to automate with conventional automation solutions. In this thesis, soft robotic end effectors are explored as a potential means of harvesting on regenerative (as well as conventional) farms. Three end effector designs are testing for parameters including grasp variability, grasp effectiveness and real-world simulation on apple orchards at Michigan State University. Apple harvesting metrics including detachment force, diameter and weight have been collected for one hundred early harvest Spartan-Macintosh variety apples. Results of this evaluation show promise for the application of these low-cost technologies; however, much work is needed before a complete and viable soft robotic harvesting system is available.

This thesis is dedicated to my parents, Kurt and Denise, and my two sisters, Alex and Maddie.
Thank you for believing in me.

ACKNOWLEDGEMENTS

I am grateful to the many individuals who have help and encouraged me during this project. I would especially like to thank:

- Dr. Ronald Averill, for his guidance, feedback, support, and advice. Without you none of this would have been possible.
- My committee: Dr. Tamara Reid Bush, Dr. Ranjan Mukherjee, and Dr. Changyong Cao.
- Phil Hill, for his generosity in allowing me to utilize his workshop.
- William Chase, for allowing me to harvest apples in the orchard.
- Mechanical Engineering main office staff
- Engineering machine shop staff, particularly Roy Bailiff and Mike Koschmider.

TABLE OF CONTENTS

LIST OF TABLES

LIST OF FIGURES

KEY TO ABBREVIATIONS

$C(\theta)$ - Total contraction function

$F_{output}(\theta)$ - Net force output

$F_e(\theta)$ – Skeleton's elastic force

L_0 - Half void opening length

k_s – Void wall stiffness

N - Number of units

D - Wall length

μ - Substitution term,

S_0 - Half of the arc length from the original parabolic approximation

h_0 - Measured depth of the parabolic approximation before contraction

Chapter 1: Introduction

The aim of this research is to evaluate the potential for the use of a soft robotic effector that is low-cost, energy efficient, simple to manufacture and appropriate for use by small-holder sustainable farms for produce harvesting. This chapter discusses the motivation for this project, including the increasing necessity of sustainable farms and food production, the issue of food security and the role of labor shortages. A review is provided of the recent developments in low-cost, simple-to-manufacture soft actuator systems. Soft robotic effectors are then presented as a potential solution for increased growth of sustainable agriculture systems. Apple harvesting in Michigan is the focus for this thesis; however, the technology could easily be applied to a variety of produce.

1.1 Small-holder farms / Regenerative farming system

1.1.1 Contemporary State of Agriculture in America

With global population on the rise and a smaller number of farms, modern agriculture has many challenges to face. By 2050 the global population is expected to exceed 9 billion people. Global food production would need to increase roughly 70 percent to accommodate the influx of consumers [1]. The United States will not see the same population influx as developing countries. Nevertheless, estimated U.S. population growth of 98.1 million from 2014 - 2050 translates to a significant increase in agricultural production needed to support the American consumer [3]. The increased strain on the American agricultural complex will have two distinct effects. First, an increase in population also means an increase in urbanization. Americans are moving away from rural areas and into cities and urban regions. As of 2016, 81.78 percent of the population in the United States is living in urban areas with an estimated 87.4 percent urban

occupation by 2050 [4] [5].

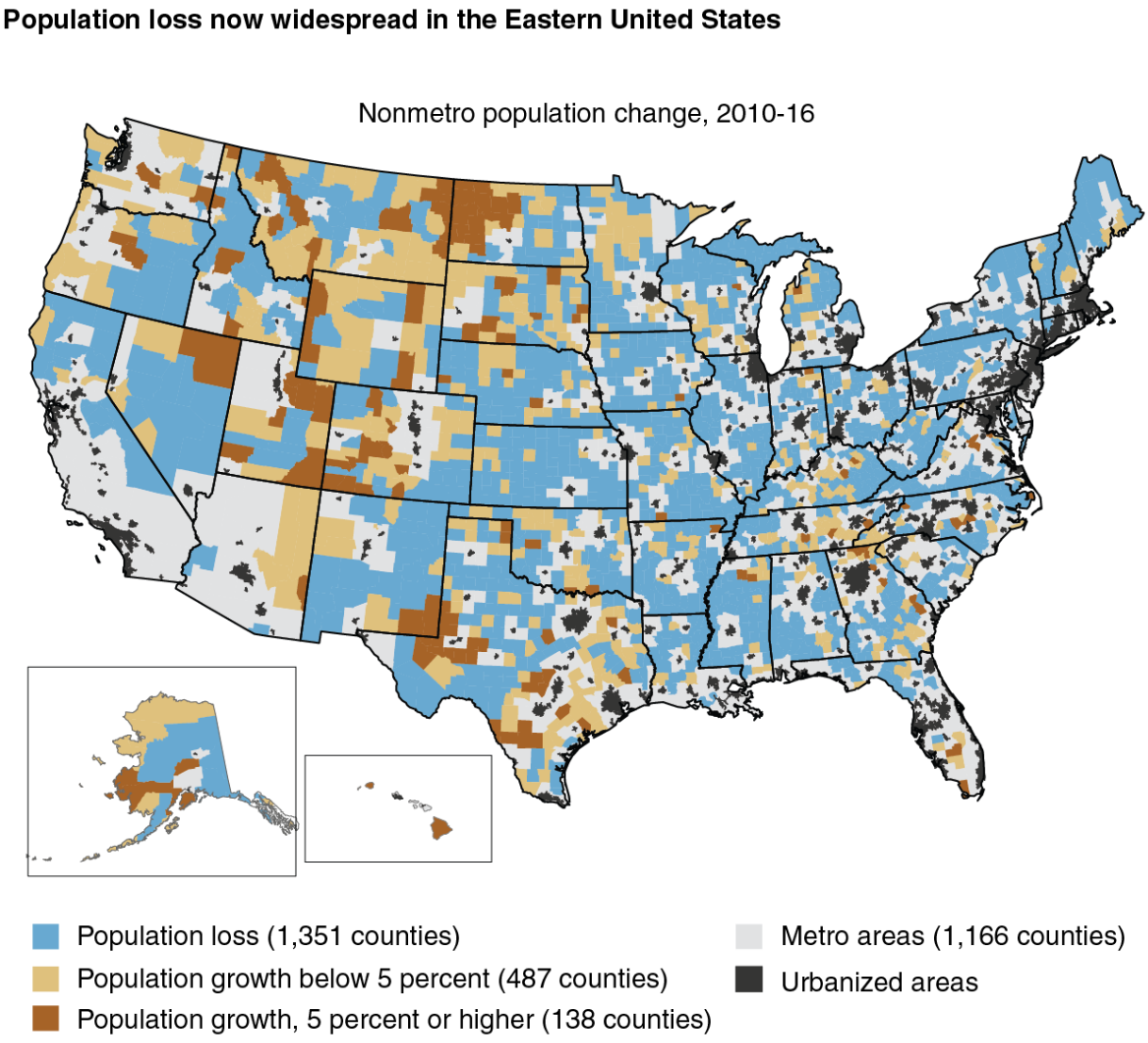

Figure 1. Map showing increasing urban immigration within the United States [6].

While urbanization has had an effect on the cost and availability of farm land, it has been shown that urban sprawl has been on the decline since 2012 [7]. A declining rate of urban sprawl and a conscious effort to design appropriate urban spaces benefits farmers through rural land prices and conservation, but does nothing to stem the flow of agricultural laborers, both skilled and unskilled, from rural to urban areas.

Second, the degradation of natural resources and remaining farmland through unsustainable farming practices is a growing concern. Estimations suggest that, with current farming practices, top soil erosion is occurring at a rate of 1.73 billion tons per year (measured in 2007), and while this is a decrease from the estimated 3.06 billion tons per year in 1982, it is still representative of practices that cannot sustain the growing population [8]. Contemporary monoculture farms, while highly labor efficient, degrade the ecosystem through the use of agrochemicals, unsustainable tillage practices, minimized diversity of plant and soil life, and deforestation. Transitioning to more regenerative farming practices will allow for more harmonious and sustainable agricultural production methods to meet the demands of the growing generations. According to a FAO, study, 73% of the world's farm holdings are small-holders, consisting of 2.5 acres or less [2]. With such a high number of farming considered "small-scale" it will be important to build a foundation of sustainability through technology that will allow these small-scale farms to flourish.

1.1.2 Farming Structures

Current agricultural practices can be separated into two categories: industrial and sustainable agriculture. Industrial, as the name suggests, represents commercial farming operations. Industrial agriculture in generally known for utilizing techniques such as monocultures, tillage fields, simple crop rotations, herbicides, pesticides, synthetic fertilizers and genetically modified (GMO) crop varieties [9]. Industrial farms can also be defined as farms which generate positive net income and require an operator on a full time basis [10]. As of 2012, 61.9% of farms in the United States contained over 50 acres of land and produced more than $54,000 per farm, with larger farms over 2,000 acres producing 1.5 million dollars [11].

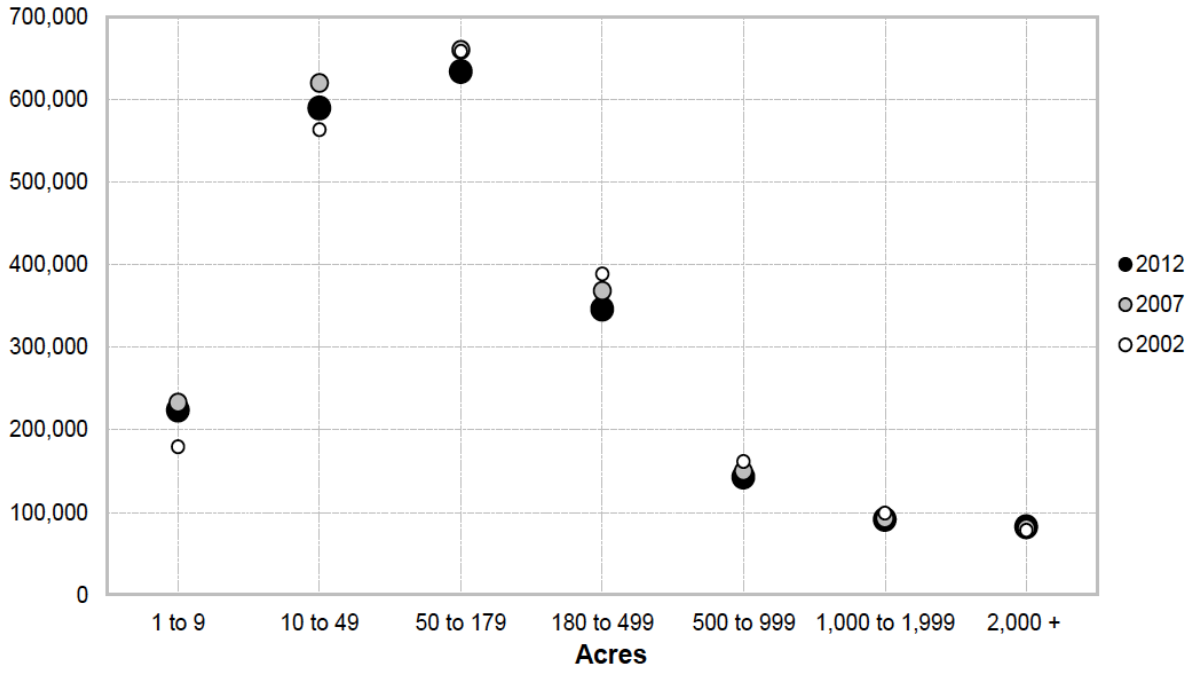

Figure *2*. Number of *US* farms by size in acres between 2002 and 2012 *[11]*.

The term "sustainable agriculture" was utilized after the World Commission on International Environment and Development created the report *Our Common Future* in the late 1980s [12]. The report utilized *Sustainable Development* as a key concept and the term *sustainable* was adopted by those in agriculture using the term *alternative-agriculture* to define methods of farming better suited for the global socio-environmental enhancement [13]. Sustainable agriculture is used mainly as an umbrella term to encompass a variety of other styles of farming. The main methods or schools of thought that will be discussed include: Organic farming, agroecology, permaculture, and regenerative agriculture.

Organic Farming, according to the 1995 USDA National Organic Standards Boards, can be defined as the following, "Organic agriculture is an ecological production management system that promotes and enhances biodiversity, biological cycles and soil biological activity. It is based on minimal use of off-farm inputs and on management practices that restore, maintain and enhance ecological harmony" [14]. Organic production systems can include the use of cover

"crops, various manures and crop rotations to fertilize the soil, maximize biological activity and maintain long-term soil health" [14]. Pests and weeds are managed through the use of biological control methods. Organic farming seeks to reduce the amount of off-farm inputs and completely eliminate the use of synthetic chemicals such as pesticides, herbicides, hormones and antibiotics.

Agroecology attempts to connect ecology with agriculture mainly with respect to the developing world. "Agroecology continues to have ecology as its basis and a focus on farm, village level, and bioregional systems. Over time, it has sought to include broader and more interdisciplinary concerns, such as analyses of how land tenure, market and trade structures, and social inequalities interact with farming systems" [15] [16].

Permaculture was developed by Australian Bill Mollison and his student David Holmgren. It "combines ecosystems-based models with landscape design processes to develop farm-level systems that integrate household systems with multistory and genetically diverse tree, shrub, and ground crops, as well as aquacultural systems" [15]. While Agroecology utilizes agricultural knowledge from historical systems, Permaculture attempts to integrate small production systems with the surrounding topography and surrounding resources.

Regenerative Farming is a broader term that is defined by the desire to understand how to regenerate not just local cropping systems, but also the surrounding value chain, including families, communities, landscapes and regions that interact with the farming community [15]. In 2017, the Carbon Underground and Regenerative Agriculture Initiative at the California State University partnered with Unilever, General Mills, MegaFood, and many other companies to develop verification standards for growing food in a regenerative manner. The Carbon Underground defines regenerative agriculture as a "holistic land management practice that leverages the power of photosynthesis in plants to close the carbon cycle, and build soil

health, crop resilience and nutrient density" [17]. Regenerative Agriculture has recently replaced sustainable agriculture as the umbrella term to describe the above alternatives to industrial agriculture. Practices such as contributing to soil health and fertility, increased water retention and safe runoff, increasing biodiversity and ecosystem health, and inverting the carbon emissions are all concepts deeply rooted in these schools of thought; however, it is the method by which these concepts are achieved that separates the four schools of thought.

1.1.3 Labor/harvesting

Nationally, the United States is dealing with a labor deficit. Between 2002 and 2014 the supply of workers available to farmers in the U.S. dropped by over 20 percent. The number of migrant labor has also dropped by over 75 percent between 2002 and 2012 [18]. While the available labor force is dropping, the subsequent generation is doing little to replace it. From 2002 to 2014, US-born farm workers offset only three percent of the decline in field and crop workers spurred by the lack of immigration [18]. A 2012 study found that 27% decline in available labor cost 3.3 billion dollars in unmet GDP growth, and 1.3 billion dollars in lost farm income [19]. Organic farms are also suffering from labor deficits. In 2006, 32% of organic farms surveyed in California reported insufficient access to labor at some point during the 2006 growing season [20]. The business structure of organic farms can also limit their access to labor. While organic farms often pay higher wages, they do not provide benefits such as healthcare, paid time off, and housing options as frequently as Industrial farms [20]. Employment conditions have a strong correlation to retention rate among employees, with return rates rising 19% if health insurance is provided, 21% for paid leave, and 9% for no-fee housing [21].

Increasing product diversity of farms, while an important aspect of regenerative agriculture, has shown to have a higher demand for physical labor. Organic farms with one to

five crop varieties required 0.45 workers per acre, while organic farms with five or more crop varieties required 0.82 workers per acre [20]. Increasing the efficiency of the available labor will be critical in order to support the projected population growth, while also meeting the defined goals for regenerative agriculture.

Automated harvesting through the use of robotics is already taking place in industrial agriculture; however, the scale at which these systems are developed are not always appropriate for small-scale regenerative agriculture farms. In order to bridge the gap in profitability and productivity between industrial and regenerative agriculture, appropriately scaled automated systems must be developed to fill the void left by an insufficient labor force. The following section will define the prerequisite knowledge for robotic harvesting systems, as well as, define the systems that will be explored as potential solutions.

1.2 Robotic effectors

1.2.1 End Effectors

End effectors or End-of-Arm Tooling are devices that attach to the end of a robotic arm and allow for interaction with the surrounding environment [22]. Robotics and end effectors have a long history of use in industrial settings since the mid-20th century [23]. In general, robotics and end effectors have been a means to alleviate stress caused by simple repetitive tasks such as pick and place operations as well as ergonomically challenging situations. Robots are commonplace in manufacturing and industrial settings, but they are now being adapted for use in agricultural settings. Planting, weeding, harvesting, and packing are all potential robotic applications that alleviate the ergonomic stresses of agricultural labor, and many other applications are possible as well.

1.2.2 Contemporary Robotic Harvesting

Produce harvesting can be described on a spectrum from a fully manual to a fully automated system. A variety of systems are being developed that are meant to aid in production such as the FRAIL-bots, currently being developed by Vougioukas et al. [24] as a means of maximizing harvesting efficiency. FRAIL-bots do this by transporting full loads of strawberries from the harvesting station to the unloading station.

Figure 3. Fragile Crop Harvest-Aiding Mobile Robots (FRAIL-bots) [24].

Another example of partial automation or automated assistance harvesting is in the form of harvesting platforms for apple picking. Lu et al. [25] evaluated commercially available

platforms, and present their own development of the self propelled apple harvester and infield sorting machine.

Figure 4. Apple harvesting and infield sorting machine designed by Lu et al. [25].

To bridge the gap between partially automated harvesting systems and fully automated systems, a means of extracting the fruit or vegetable from the plant is necessary. This will require an end effector. Challenges in designing end effectors for produce harvesting include: canopy avoidance, collision avoidance, assessing desirability of produce, secure grasping while minimizing bruising and extraction of the fruit from the plant. There has been significant research into the development of an end effector for robotic apple harvesting. Bulanon et al. [26] developed an end effector and robotic vision system in which the apple is grasped at the peduncle as opposed to the fruit body. One advantage to this design is the low profile of the end effector; however, accuracy require to grasp the peduncle was discussed as an issue in the

literature. Davidson and Silwal developed an under-actuated end effector used in conjunction with a vision and base system [27].

Figure 5. End effector and harvesting platform [27].

Robotics company, FFRobotics, is developing a fully autonomous harvesting system and is competing against Abundant Robotics to be the first to commercialize a robotic apple harvesting system [28]. The advantages of these system is their fast harvesting speeds, however, they require the apple orchards to be arranged in a specific manner to best utilize either platform.

Figure 6. On the Left FFRobotics End Effector harvesting system and on the right is the vacuum harvesting system from Abundant Robotics [28].

Contemporary end effectors discussed in this section have many advantages; however, many lack energy efficiency, are difficult to manufacture, and are too expensive for small-scale regenerative farmers. In the following section, soft robotics will be discussed as a cost effective replacement for contemporary end effectors.

1.2.3 Soft robotic end effectors

Soft robotics are a category of machines created from compliant materials such as elastomers, polymers, hydrogels, and granules. They are driven by either pneumatics, electricity or chemically [29]. Soft robotics and specifically soft end effectors have become an active area of research due to their safety with regards to human robot interaction, energy efficiency, low cost and resilience [30]. Soft grippers have gained interest as a means of produce handling for the reasons stated previously, as well as their ability to gently grasp the produce without causing bruising or damage. Soft pneumatic actuators (SPAs) are a well developed category and have seen much progress since their development. Pneumatics, especially when using air as the fluid, offers many advantages including: rapid inflation due to the low viscosity of air, pressurized air is easy to control, readily available, and can be discarded through venting after use [29]. While chemically driven actuators do not require the bulky compressors and vacuums that SPAs do, the

technology needs further development before it can produce a commercially viable actuator. The Silicone-ethanol elastomer presented by Miriyev et al. [31] utilized the reaction between the joule heating element and the ethanol voids which vaporizes and expands the silicone matrix. This novel approach to actuation requires much less supporting equipment when compared to SPAs; however, the rapid degradation of the actuator makes it incompatible with the requirements for an agricultural end effector. The following section will describe the styles of elastomer soft actuators that will be considered as potential end effectors for use in soft robotics

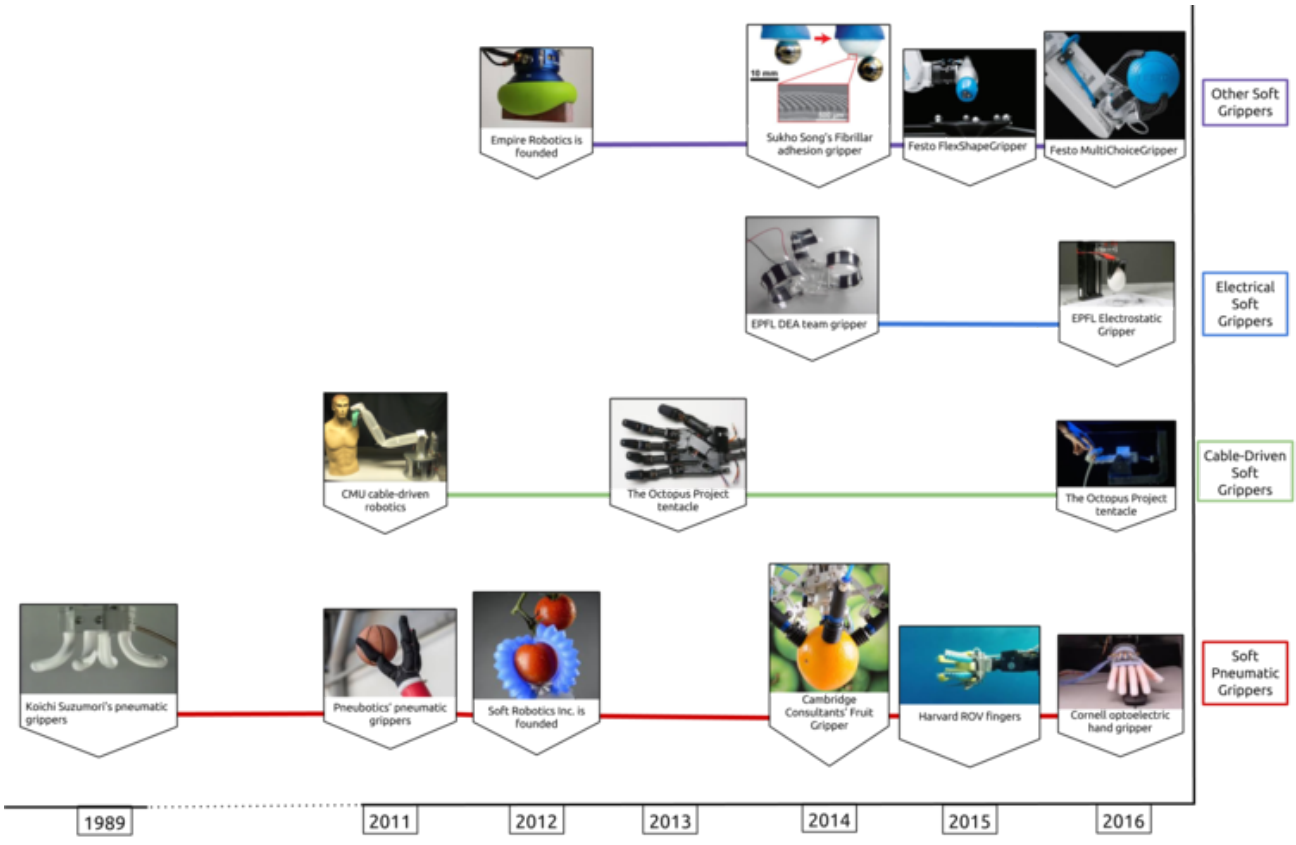

Figure 7. Timeline of notable soft grippers [32].

1.2.3.1 PneuNets

PneuNets developed by Ilievski et al. is a soft robotic design that utilized a network of embedded pneumatic channels within an elastomer body [33]. The repeated channels inflate and deform the elastomer like a balloon. Requiring only a single source of pressure the channeled elastomer is combined with an inflexible bottom layer. When used in conjunction, the inflexible bottom layer "directs" the inflation upwards through the elastomer and produces the curvature, as seen in **Error! Reference source not found.**.

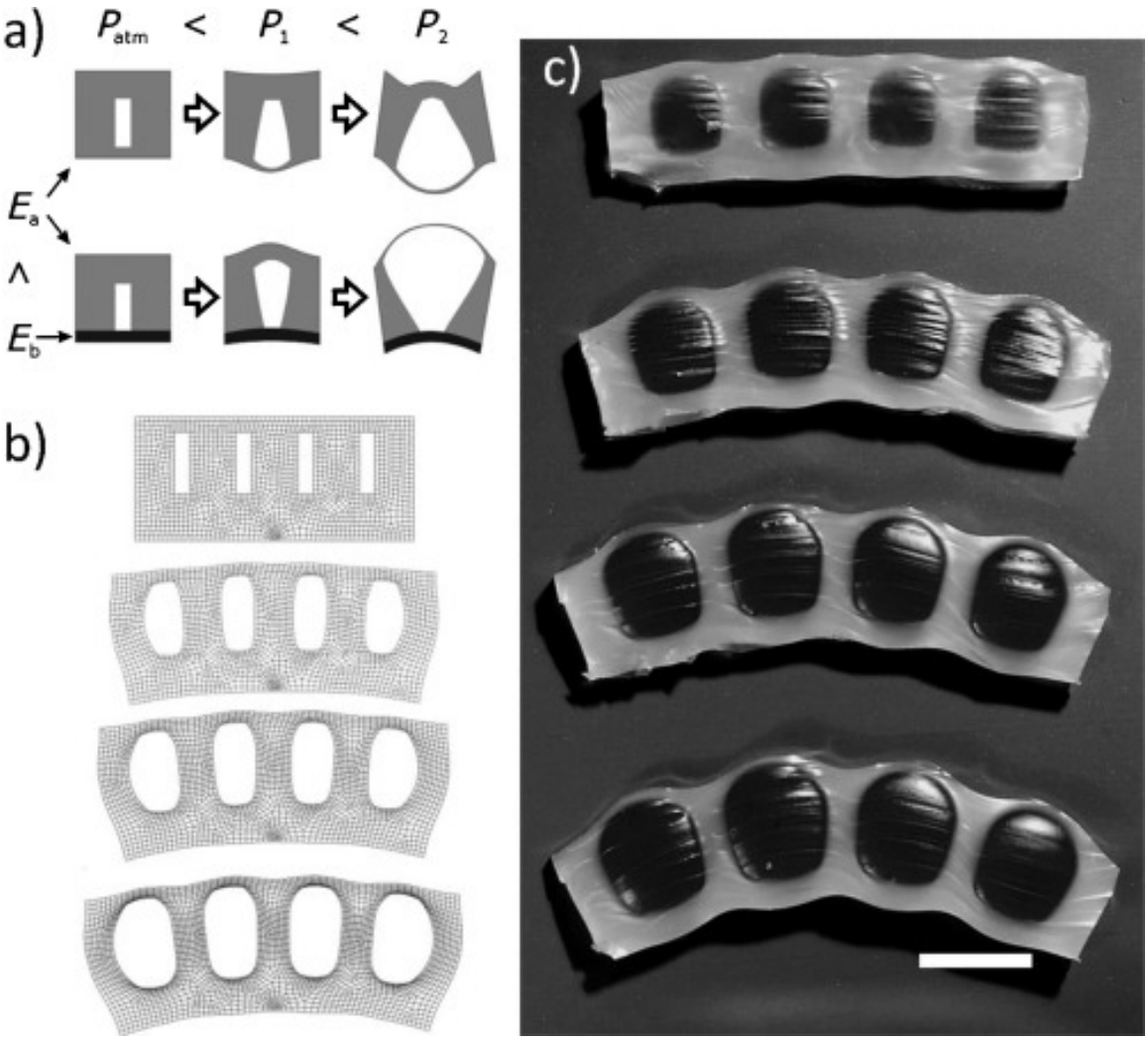

Figure 8. a) showing comparison between elastomer expansion and expansion with elastomer and inflexible layer. b) FEM of elastomer with inflating channels. c) sectional slices of pressurized channels [31].

.

1.2.3.2 FOAM

Fluid-driven origami-inspired artificial muscle (FOAM) is a sub category of soft actuator or artificial muscles developed by Robert J. Wood and his coworkers [34]. The actuator is made up of three components: a folded skeleton, a TPU flexible skin, and a means of connecting the device pneumatically. Actuation is driven by the folded skeleton, while the skin provides the means of contractile force. While the FOAM actuator can be driven with positive or negative pressure, negative pressure is safer for use in an environment where operators will be present. A variety of motions such as bending, linear contraction and torsion can be achieved based on the folding scheme imposed on the skeleton (Figure 9).

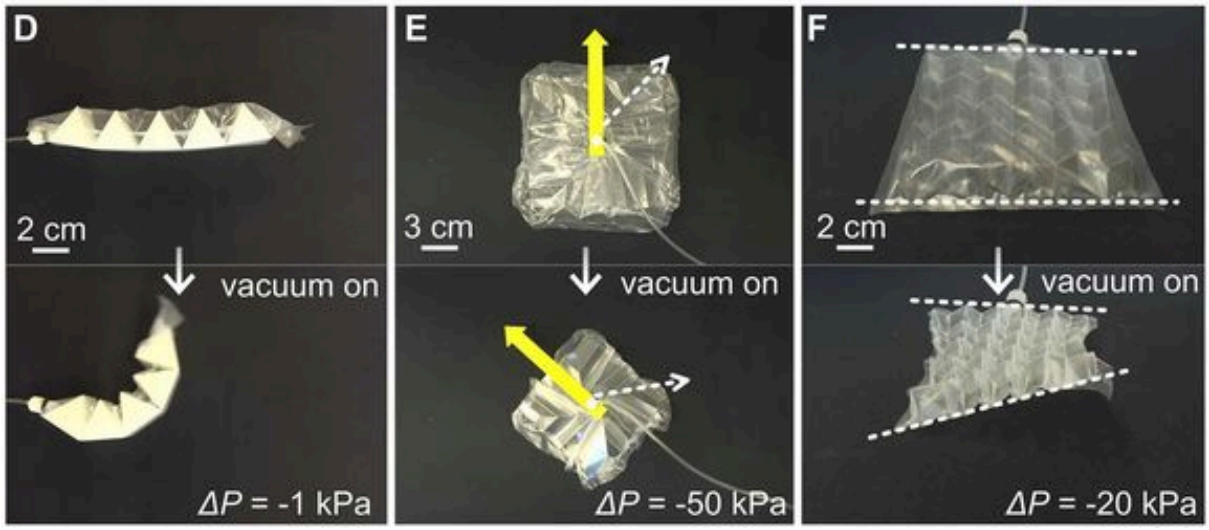

Figure 9. FOAM skeleton designs and their respective motions [34].

1.2.3.3 Optimal Gripper Design

While the grasping strategies for the FOAM actuator are elegant, complex folding schemes such as the Muri fold require laser cutting to fold rigid materials. Implementing a passive gripper is one solution that would require less specialized equipment. Liu et al. [35] designed a compliant optimal gripper for grasping objects of unknown size or shape. The group utilized a topology

optimization method to create their two-finger gripper mechanism with printed flexible filament. The two-finger gripper used linear displacement to engage the gripper ends, as shown in Figure.

Figure 10. Optimally designed two-finger gripper holding a weighted cylinder [35].

1.3 Proposed Solution

As a means of increasing productivity and alleviating stress from labor shortages, it is proposed to explore the potential for soft robotics as a form of appropriate technology for regenerative farming. Soft robotic actuators and gripping systems offer many advantages to contemporary robotic effectors such as low cost, energy efficiency, operator safety, and reduced produce damage. The focus of this research will be the grasping phase of the “pick and place” task segmentation, as seen in Figure.

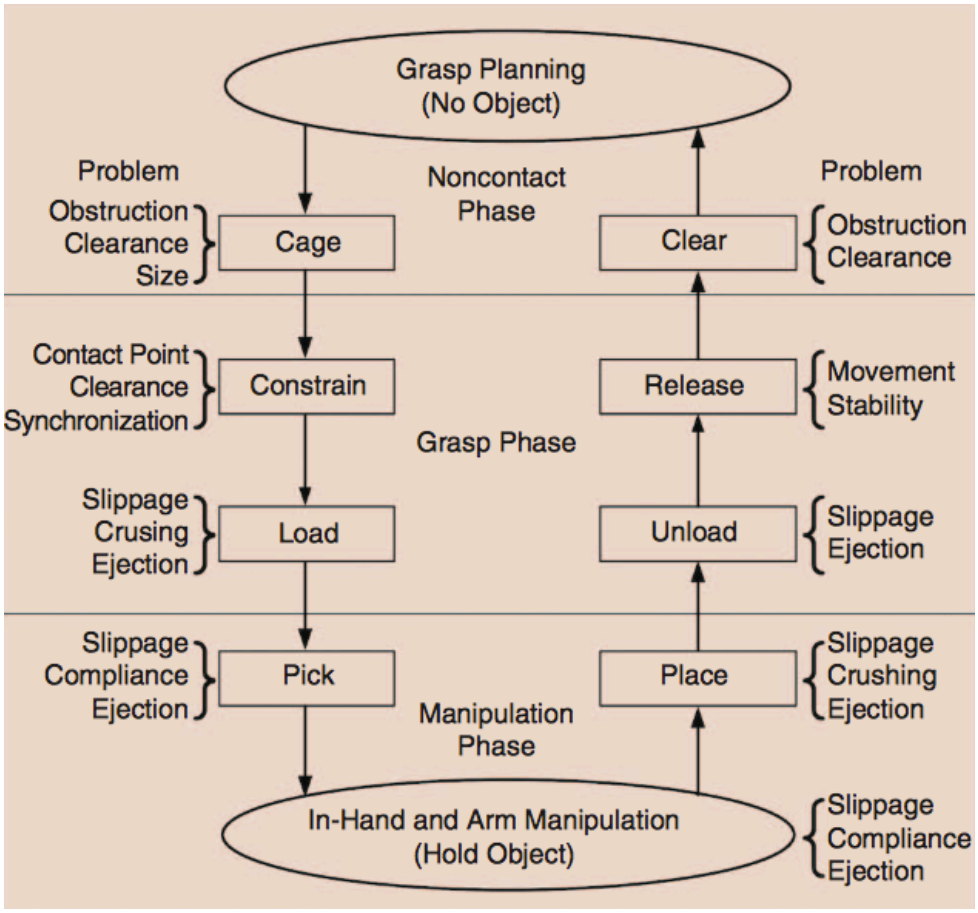

Figure 11. Pick and place task segmentation [36].

A combination of a FOAM actuator and the two-finger gripper system will be explored as a potential low-cost end effector for use in regenerative farming produce harvesting. Linear contraction will be provided by a FOAM actuator and enable the grasping mechanics of the two-finger gripper system. This design will be tested for harvesting efficiency, potential for produce damage, manufacturing feasibility, and cost effectiveness. The proposed system will be tested against alternative soft actuators such as the PneuNets and an alternative FOAM gripper for comparison.

Chapter 2: Design and Components

Three designs were selected for testing as potential soft robotic end effectors. A modified version of the optimal gripper design (Figure 10), a FOAM gripper design that utilizes the *magic-ball* origami fold pattern, and a four-finger PneuNets design based on the work of Zhang et al. [37]. While many other soft robotics designs are available, these were chosen because they met the design requirements needed for produce harvesting on regenerative farms. The primary design requirements considered here for produce harvesting on small-scale regenerative farms are as follows: simple, low-cost, safe, and functional. Functionality refers to manipulative dexterity, grasp robustness, and efficiency. Chapter 2 will describe the three selected designs, their cost and material requirements.

2.1 Optimal gripper Design

In the original paper by Liu et al. [35], the compliant optimal gripper is a two-finger system utilizing a direct current motor connected to a threaded rod via a bevel gear to provide displacement. Two appendages are the minimum required by an end effector to successfully contain an object; however, the material selected for the current study, Dragon Skin 30, is less compliant than the thermoplastic elastomer used by Liu et al. A third *finger* was added in the hopes that it would reduce potential slippage and ejection during the load phase of grasping. A three *finger* arrangement would also distribute force more evenly across the surface of the produce being harvested. Displacement in the three *finger* arrangement was produced by a FOAM style linear actuator mounted in the center. Early iterations of this design utilized a simple *zigzag* FOAM skeleton pattern (Figure 1) to produce the linear contraction; however, early trials showed the simple *zigzag* actuator was incapable of producing the necessary force before buckling.

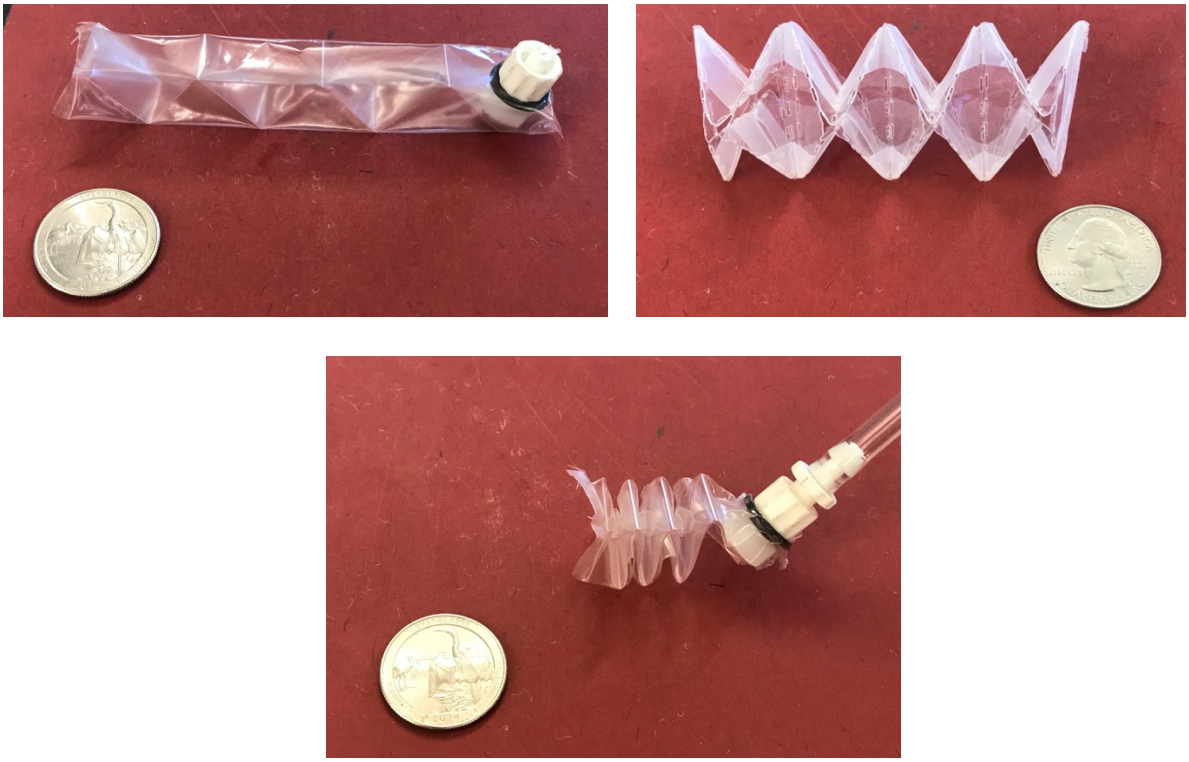

Figure 12. A simple zigzag design FOAM actuator is shown on the top left. A four segment "water-bomb" bellow "skeleton" is shown on the top right. Contracted zigzag FOAM actuator is shown on the bottom.

As seen in Figure 1, the final iteration of the three *fingered* optimal gripper design used a bellowed skeleton design which was less likely to buckle due to the 3D nature of the fold pattern. The bellowed skeleton is created from a single strip of 12 "water-bomb" base origami folds, Figure, which is then folded in half with the seams bonded. Material for the skin and pneumatic fittings are the same for the bellowed skeleton as in the zigzag design.

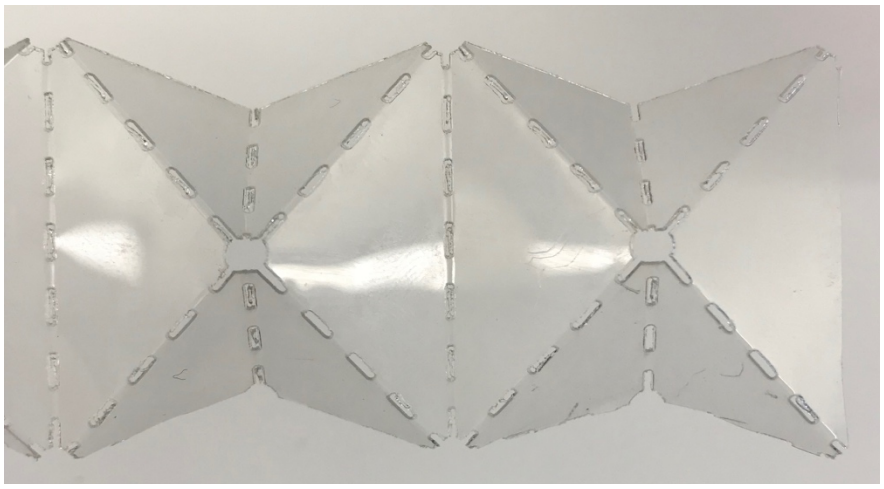

Figure 13. Two sections of "water-bomb" base folds.

For the final prototype of the optimal gripper design, the actuator and the *fingers* are connected by two printed PLA rings with the actuator mounted between two “T” shaped PLA cross members. A wafer component was added to restrict the motion of the “T” shaped cross member during contraction. Details of the three *fingered* optimal gripper design can be seen in Figure .

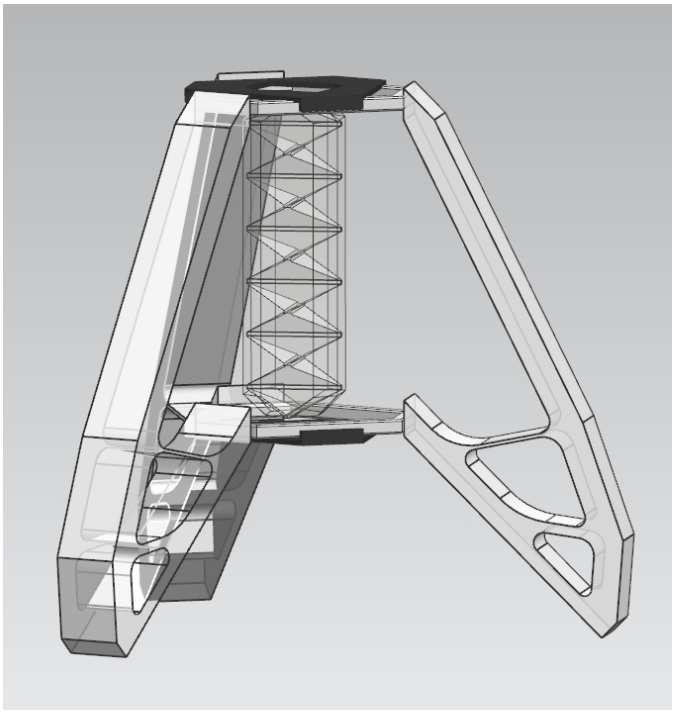

Figure 14. CAD model of optimal gripper.

Figure 15. Functional prototype of optimal gripper design.

Modeling of the optimal gripper design has been evaluated with FE analysis and through prior analytical modeling developed by Li et al. Actuation by the FOAM linear actuator can be modeled as a two hinged ridged beam with an opening angle of 2θ. The hinge itself can be shown as two cantilever springs [34].

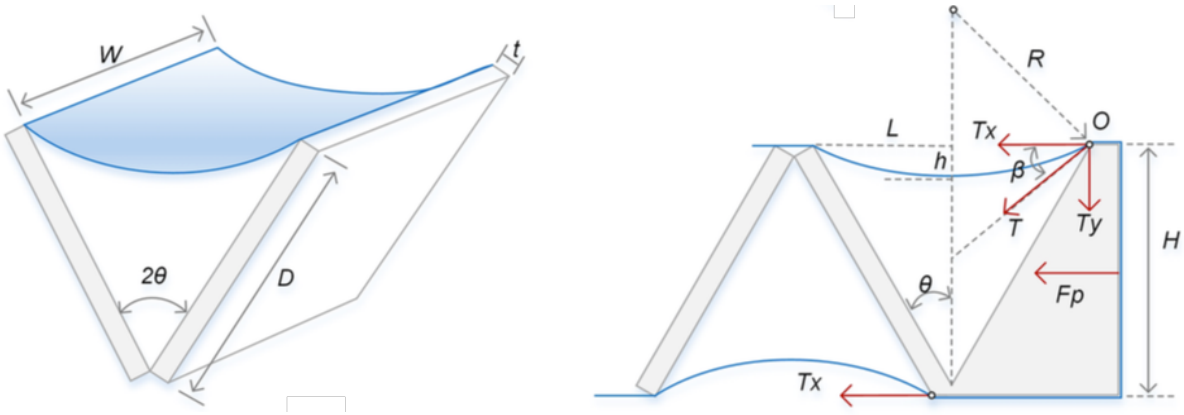

Figure 16. Hinged plate model shown left with the force balancing model shown right.

Total contraction of a linear zigzag skeleton FOAM actuator can be modeled as

$$C(\theta) = 2ND(\sin\theta_0 - \sin\theta) \quad (1)$$

Where N is the number of units and D is the wall length shown in Figure. Net force output for a linear zigzag FOAM actuator can be estimated as

$$F_{output}(\theta) = 2\big(F(\theta) - F_e(\theta)\big) \quad (2)$$

where F(θ) is the force function and $F_e(\theta)$ represents the skeleton's elastic force, and can be calculated by the equation

$$F_e(\theta) = k_s(L_0 - D\sin\theta) \quad (3)$$

$$k_s = \frac{EWt^3}{4D^3} \quad (4)$$

where L_0 is half the void's opening length shown in the force balancing model in Figure. Bending stiffness of the void walls, k_s, includes the tensile modulus of the skeleton material, the width and the thickness. F(θ) can be predicted as [34]:

$$F(\theta) = -\frac{\Delta PW}{2}\left(\frac{D\left(cos^2\theta - sin^2\theta\right) - \lambda(\theta)\left(\mu^{\frac{1}{2}}cos\theta - \mu^{-\frac{1}{2}}D^2sin^2\theta cos\theta\right)}{cos\theta}\right) \quad (5)$$

$$\lambda(\theta) = 1 + \frac{(\theta_0 - \theta)\left(\frac{D}{S_0} - 1\right)}{\theta_0} \quad (6)$$

$$\mu = S_0^2 - D^2sin^2\theta \quad (7)$$

$$S_0 = \frac{1}{2}\left(\left({L_0}^2 + 4{h_0}^2\right)^{\frac{1}{2}} + \frac{{L_0}^2}{2h_0}\sinh^{-1}\left(\frac{2h_0}{L_0}\right)\right) \quad (8)$$

$$L_0 = D\sin\theta_0 \quad (9)$$

where λ(θ) is the linear correction term necessary because the previous force function did not approach zero when the voids were completely closed (θ = 0). Due to an inaccurate approximation of the fluid volume, the correction term is needed. μ is used as a substitution term, S_0 is one half of the arc length from the original parabolic approximation, h_0 is the measured

depth of the parabolic approximation before contraction, and L_0 is half the void's opening length [34]. A simple finite element model was built using software package NX 10.0 for the 3D printed components of the optimal gripper design.

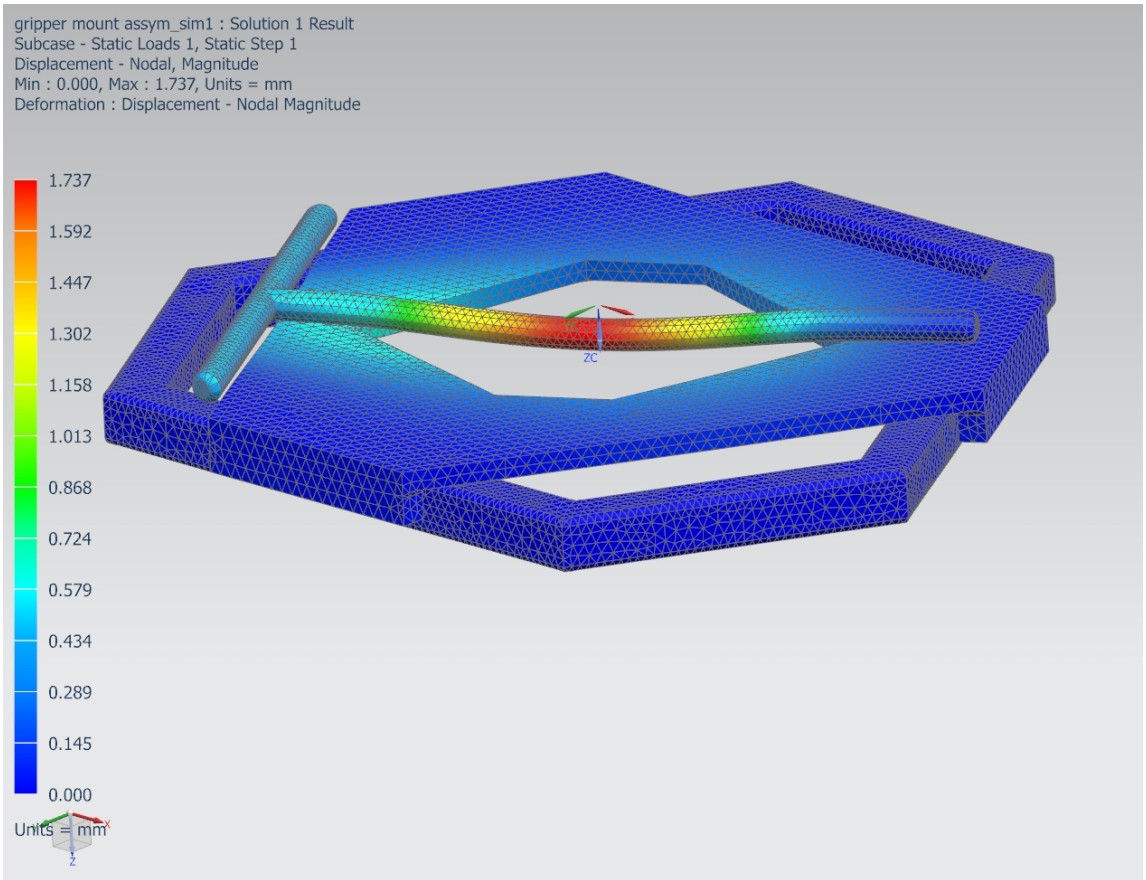

Figure 17. Finite element model for 3D printed components of optimal gripper design.

The model shown in Figure was generated by fixing three arms of the triangular ring where the Dragon Skin *fingers* were to be mounted. A distributed load was simulated over the T-shaped pin. The three components were combined under surface-gluing constraint. The resulting simulation shows that the current design will function within the prescribed load limits. This simulation did not take into account the complexities of layer by layer FDM printing which could produce a weaker structure. Finite element modeling has also been done for the compliant optimally designed fingers. The simulation was included in the paper by Liu et al. [35], and

shows equivalent stress contours for one finger under displacements of 33 and 50 millimeters contacting a sphere of 45 millimeter radius. Liu et al. measured the elastic modulus of their flexible filament and it was found to be 11.6 MPa.

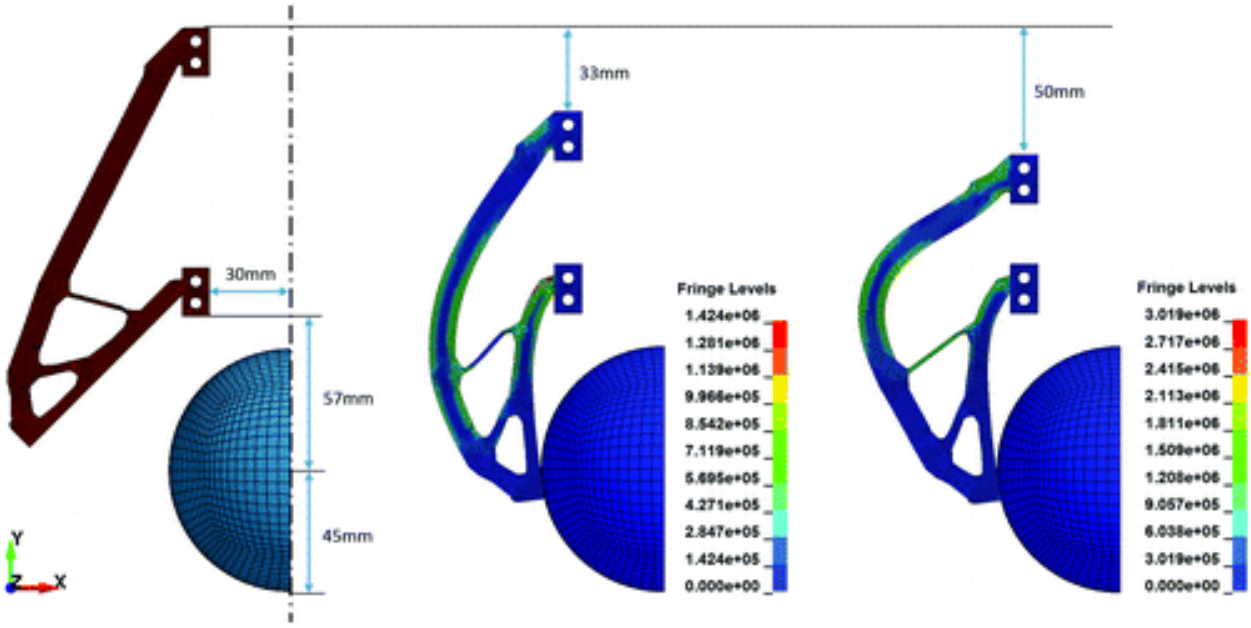

Figure 18. Finite element model of optimal finger from the research of Liu et al. Stress contours are shown in MPa [35].

2.2 FOAM Magic-Ball

The Magic-ball Origami fold is derived from the “water bomb” base folding unit. From the original design presented in the paper by Liu et al. [34], the only alteration made was an increase in scale to better encapsulate larger objects. Although fold layout is dimensionless, the figures in the original paper show the original design by Li et al. as approximately 9 centimeters in diameter.

Figure 19. Water-bomb skeleton fold from Li et al [34].

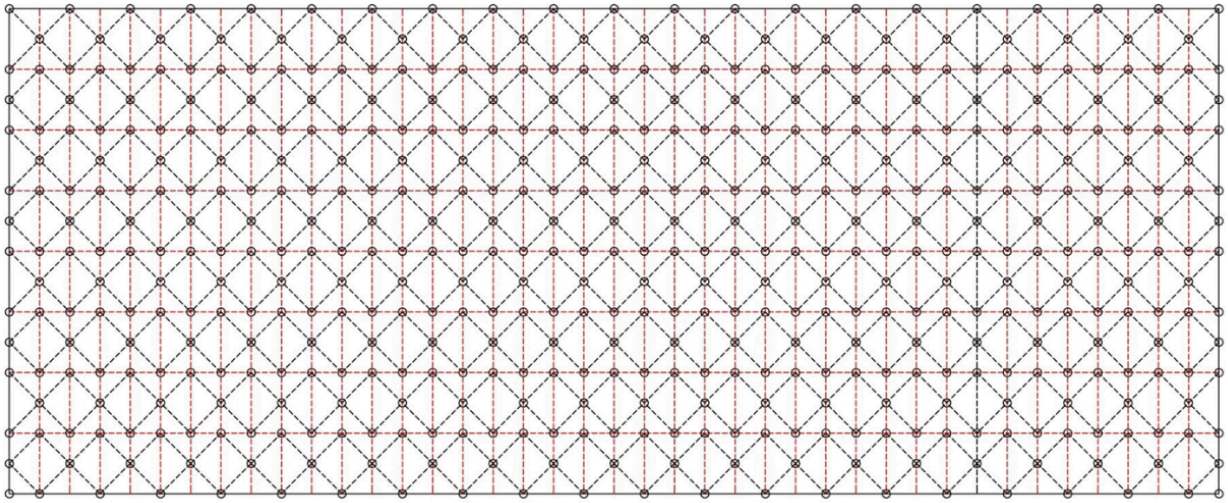

Figure 20. Magic ball fold patterned used by Li et al [34].

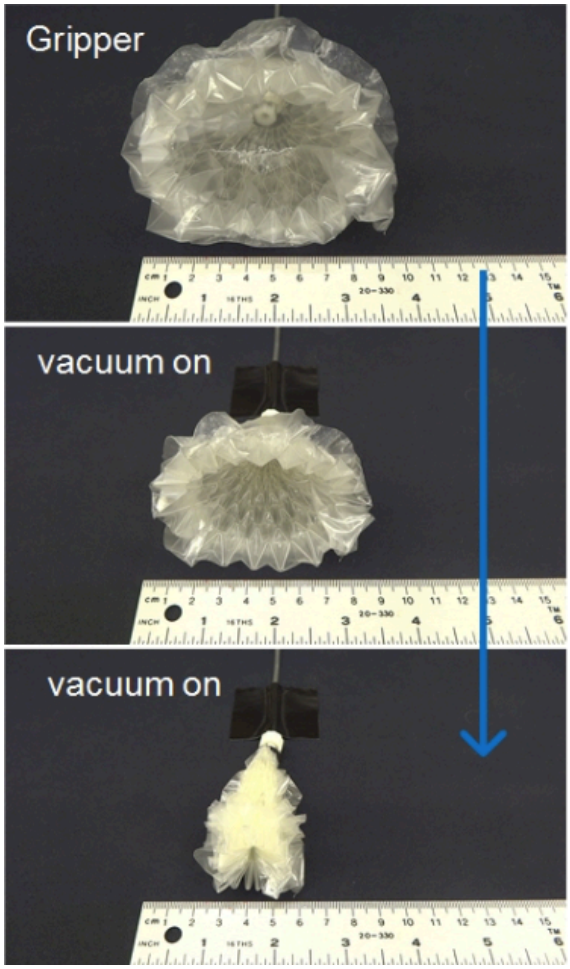

Figure 21. Functionality of the "magic-ball" gripper can be seen as a vacuum is turned on and air is removed [34].

Figure 22. Scaled "magic-ball" gripper design. Skeleton shown left, skeleton with skin shown right.

2.3 PneuNets Design

As described in section 1.2.3.1, PneuNets, designed by Ilievski et al. [33], has been utilized in a variety of designs. In the original paper, Ilievski et al. described a six limbed “starfish-like” design cast from two parts elastomer between one strain-limiting layer.

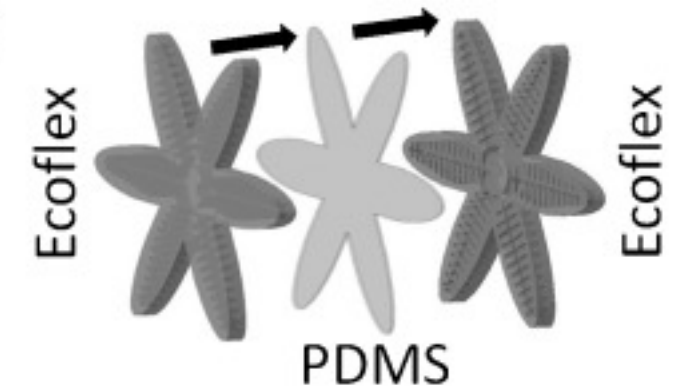

Figure 23. "Starfish-like" design by Ilievski et al.

This “starfish-like” design is capable of contracting in both directions given the symmetrical nature of the design. Further developments by Mosadegh et al. [29] in 2014 created an alternative design called fast pneu-net (fPN) with the original design being referred to as slow or simple pneu-net (sPN).

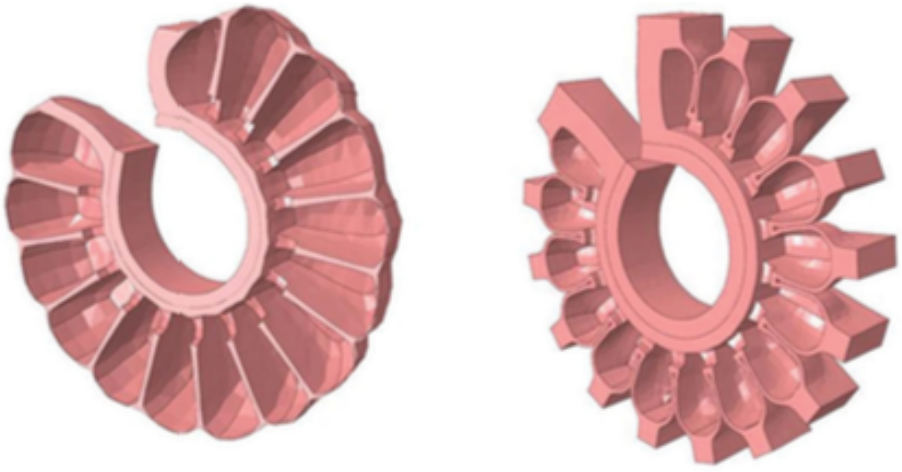

Figure 24. Original sPN design on the left with the fPN shown on the right [29].

fPN actuators have various performance benefits over sPN including, significantly faster actuation speed (25x sPN) and reduced change in volume. Drawbacks of the fPN design include deflection under gravity due to hinge like structure and a non-linear bending when pressurized above their full bending amplitude [29]. Companies such as Soft Robotics Inc. have taken designs similar to fPN and commercialized them for pick and place automation [38].

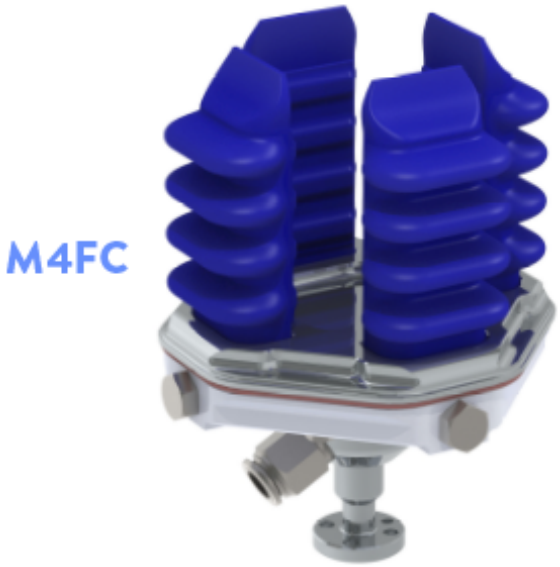

Figure 25. Four actuator configuration from Soft Robotics Inc. [38].

For use in a regenerative farm setting, a simple pneu-nets configuration was selected. Simplicity of manufacturing, cost and compliance were factors affecting this decision. Based on the design from both Ilievski et al. [33] and Zhang et al. [37], the design, presented in Figure and Figure, uses a four *finger* grasping strategy composed of a cast of elastomer material adhered to a layer inelastic material. An air line is inserted and sealed on top of the device.

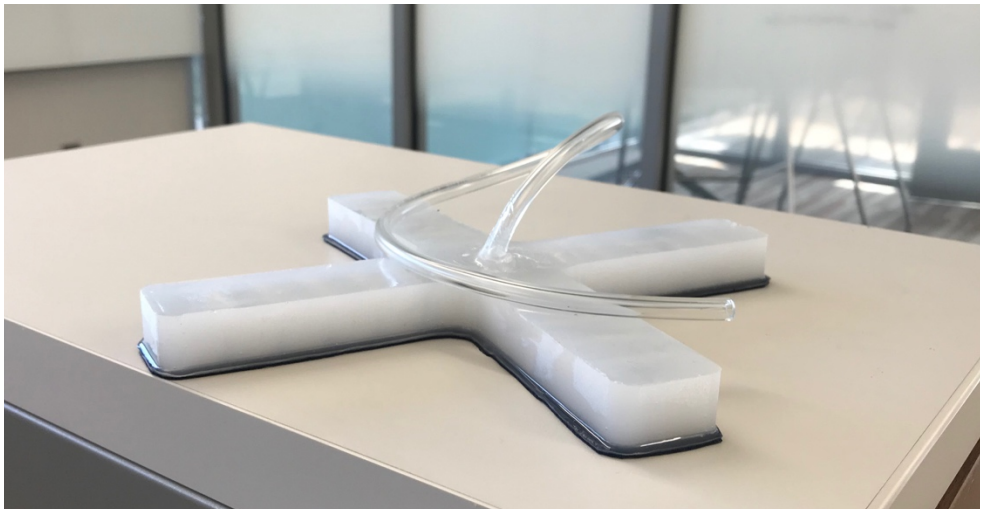

Figure 26. Pneu-Nets design unactuated.

Figure 27. Pneu-Nets design actuated and grasping 3.75" diameter sphere.

2.4 Cost and material selection

Table 1. Cost of materials and manufacturing.

		Part	Material	quantity	cost
Optimal Gripper design	Components	Gripper finger	Dragon Skin 30	3	$5.04
		Triangular ring	PLA	2	$1.00
		T shaped pin	PLA	2	$1.00
		Wafer support	PLA	2	$1.00
		Actuator skeleton	polyester sheet	480 x 40mm	$0.17
		Actuator skin	polyurethane film	~ 140 x 120mm	
		Actuator fittings	Nylon nut	1	$0.07
			Rubber washer	1	$0.43
			Nylon quick turn coupling	1	$0.55
				Component Total	$9.26
	Manufacturing	3D printed gripper mold	PLA	1	$7.00
		3D printed bonding mold	PLA	1	$2.00
		Laser cutting	-	1	$2.00
				Manufacturing Total	$11.00
				Design Total	$20.26
Pneu-nets design	Components	Main body cast	Eco-flex 00-30	1	$7.39
		Inflexible layer	Cotton sheet	200 x 200 mm	$0.05
		Air hose	1/8 inch ID 1/4 inch OD PVC tubing	~350mm	$0.15
				Component Total	$7.59
	Manufacturing	3D printed Main body mold	PLA	1	$8.00
				Manufacturing Total	$8.00
				Design Total	$15.59
Magic Ball design	Components	Actuator Skeleton	Polyester sheet	230 x 460 mm	$0.92
		Actuator skin	polyurethane film	80424mm^2	
		Actuator fittings	Nylon nut	1	$0.07
			Rubber washer	1	$0.43
			Nylon quick turn coupling	1	$0.55
				Component Total	$1.97
	Manufacturing	Laser Cutting	-	1	$13.00
				Manufacturing Total	$13.00
				Design Total	$14.97

For the Optimal gripper design, Dragon Skin 30 (from smooth-on), was selected due to its high tensile strength and 100% modulus, as well as its safety once fully cured. PLA was selected as filament for the 3D printed components because of its low cost, biodegradability, and

availability. Actuator components such as the polyester skeleton material, polyurethane skin material, and pneumatic fittings were based on materials utilized in the research by Liu et al. Eco-Flex 00-10 was chosen due to its use in the original development of Pneu-nets by Ilievski et al. and due to is material safety. All of these design are not limited to the materials listed in Table 1. For example, in the original paper by Ilievski et al., paper was first used as the strain-limiting layer of the pneu-nets design. Polydimethylsiloxane (PDMS) was later utilized due to improved performance characteristics [33]. Materials selected for this study have been done so with cost, availability, and similarity to prior art in mind.

Chapter 3: Manufacturing Methods

Manufacturing is a critical step in the design process, and often results in alterations to original designs. Processes for manufacturing the three end effectors were selected based on equipment availability, cost, and simplicity. A multiplicity of processes exist for manufacturing these actuators and end effectors; however, due to time constraints, only the methods discussed were evaluated. This chapter details the methods that resulted in successful prototypes, while still adhering to the process criteria for each of the three designs. Equipment such as fused deposition modeling 3D printers and laser cutters were available through university facilities; however, many 3D printing and laser cutting services exist online.

3.1 Optimal Gripper Design

3.1.1 Actuator Fabrication

Actuator fabrication can be broken up into three steps: skeleton folding, initial skin sealing, and fitting installation and final sealing. Fitting installation and final sealing is the last step in the optimal gripper design assembly process. To start this process, a sheet of polyester film was sent to the laser cutter with the programmed pattern seen in Figure. Cutting was done on the Full Spectrum hobby series CO_2 laser cutter. Vector cutting was used on power setting 20% with speed at 85%.

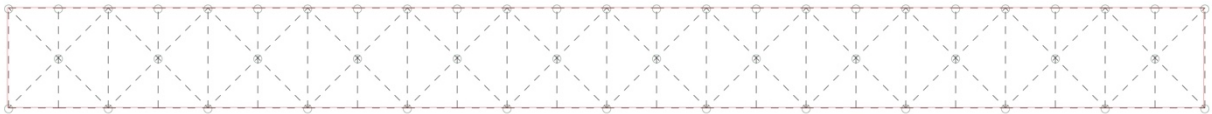

Figure 28. Strip of water-bomb base folds.

The strip is folded in half connecting the two free ends, pre-folding on the patterned cuts is recommended before connecting free sides. Polypropylene tape (packaging tape) is applied to all

three of the free edges. Fold by pushing on the top and bottom of the vertical cut lines then compress horizontally to finish the folds.

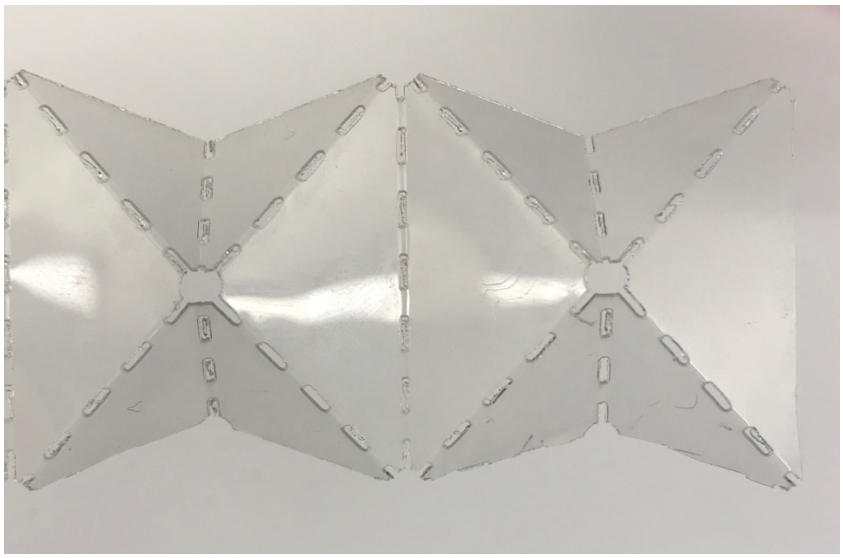

Figure 29. Single side of water-bomb base strip.

The resulting six segment bellowed skeleton should look similar to the four segment bellowed skeleton in Figure 1. Cut an approximately 140mm x 120mm rectangle of the 0.0015-gauge polyurethane film material and seal length wise around the bellowed skeleton using an impulse sealer. An AIE-305 table top impulse sealer was used on the number three dial setting for 0.0015- gauge polyurethane material.

3.1.2 3D Printing Components

Components used in this work were 3D printed by the MSU College of Engineering computing services using standard fused deposition modeling (FDM) printers with PLA filament. Printer model use was based on availability and included models such as the Monoprice MK11 and Makerbot replicator. Infill percentages for the molds was 15% using the honey comb pattern. The triangular ring, wafer and T-shaped pin were printed at 50% and 70% respectively; however, the T-shaped pin and wafer was small/thin enough they did not require any infill.

3.1.3 Gripper Finger casting

Casting of the gripper fingers required the following equipment: digital scale, disposable mixing cup and stirring utensil, Dragon Skin 30 (part A and B), painters tape, and the two printed molds. Molds are inspected to ensure they are clear of extraneous filament and debris. The two-part gripper mold is connected using the locator pins then sealed along the edge using the painters tape.

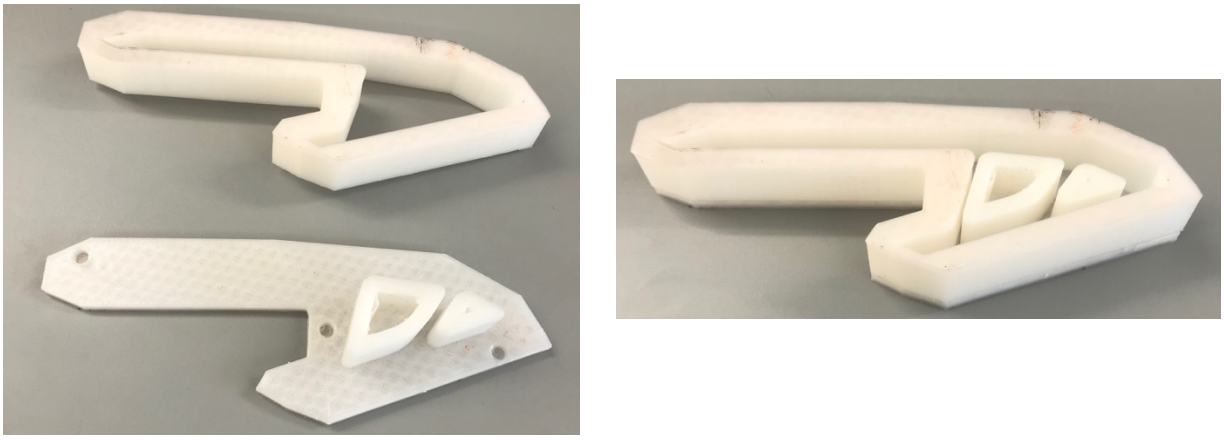

Figure 30. Two-part gripper finger mold.

25 grams of both part A and B of the Dragon Skin 30 platinum cure silicone is measured and combined in the disposable cup. After thoroughly mixing both casting parts, the mixture is slowly poured into one corner of the mold. Holding the disposable cup at a higher distance from the mold forms a thinner stream of silicone and can reduce the number of large bubbles in the cast.

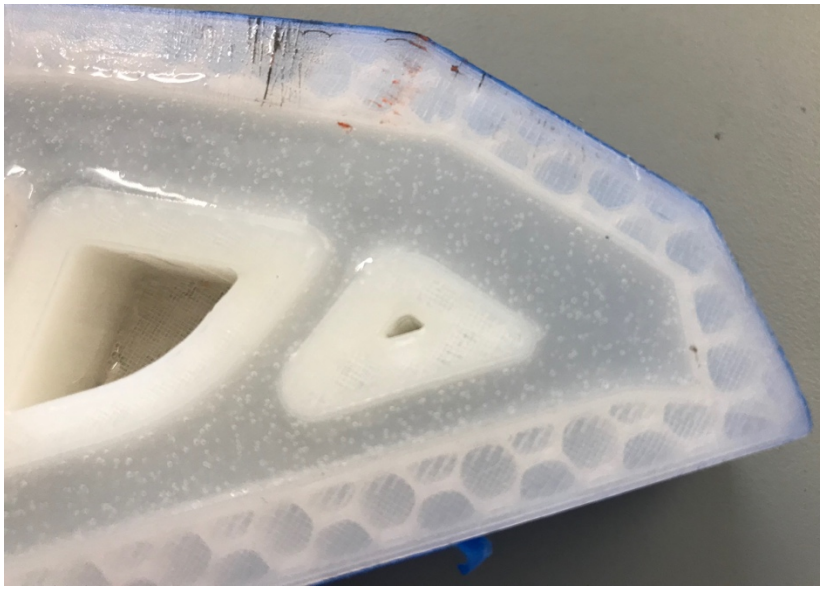

Figure 31. Small bubbles can be seen in the silicone material during the casting process.

Alternatively, vacuum degassing in a vacuum chamber eliminates bubbles from the silicone mixture prior to casting. Casts of the Gripper finger are fully cured in 12 hours. No mold release was used during the casting process. This process is repeated three times. After the three grippers have been cast, they are inserted into the connector mold along with a 3D printed triangular ring with the outer curved side of the gripper finger facing away from the center of the mold.

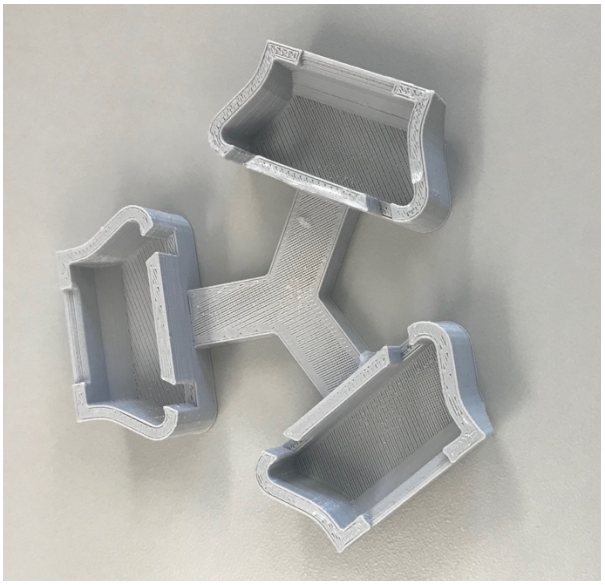

Figure 32. Connector mold.

30g of Dragon skin 30 (15g of each part) is mixed and poured into the mold with the gripper and triangular component. The notches where the triangular ring is inserted should be taped with tape so the silicone can completely fill the mold. Both the top and bottom of the gripper finger are combined with the triangular ring in this manner.

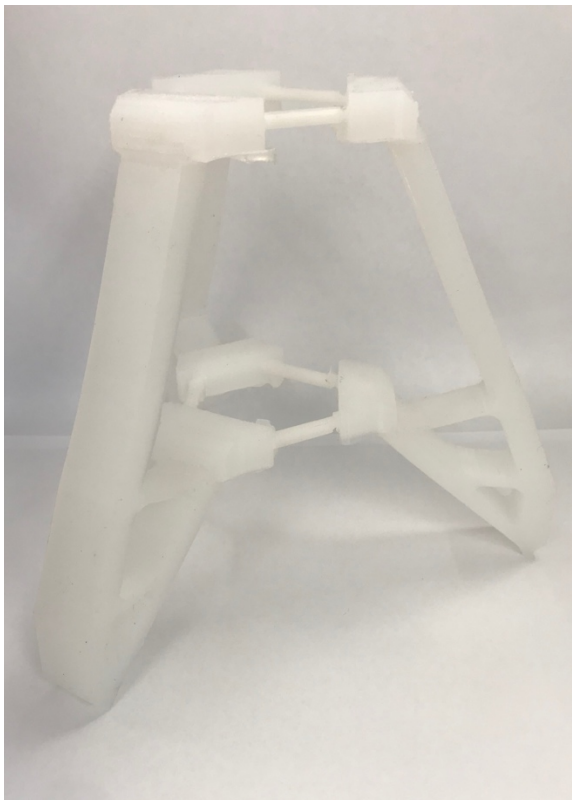

Figure 33. Three gripper fingers bonded with two triangular rings.

3.1.4 Assembly

Assembly begins by first inserting the unfinished actuator into one of the two wafer components. After the actuator is inserted into the wafer, the skin material is folded over the sides of the wafer, exposing the bellowed skeleton. Inserting the T-shaped pin into the skeleton ensures that the skeleton will not pass through the wafer during actuation. Unfold the skin material and seal with the AIE-305 impulse sealer on setting number 3. Before this process is repeated on the top

end of the actuator, the assembly must be inserted through both triangular rings in the gripper ring assembly.

Figure 34. Exposed skeleton after insertion through wafer shown on the left. On the right, the T-shaped pin inserted through the skeleton.

Before final sealing of the actuator, the pneumatic fittings should be attached to the skin material via a small incision. Once assembly is completed, the three raised edges of the wafers should hang over the edges of the triangular ring and constrain the actuator to the center of the assembly.

Figure 35. Fully assembled optimal gripper design.

3.2 PneuNets Design

PneuNets fabrication is the simplest of the three designs. However, it requires approximately 24 hours of casting time for this specific design. Required materials include: Eco-flex 00-10 platinum cure silicone, digital scale, disposable cup and mixing utensil, 3D printed top mold, cotton or equivalent, a 1/8th inch diameter nail or equivalent, and PVC tubing. First, insert the nail into the hole in the center of the 3D printed mold, this allows the tube to be inserted without cutting material after casting.

Figure 36. 3D printed PneuNets mold.

Mix one hundred grams of both part A and part B of Eco-Flex 00-10 thoroughly in a disposable cup and pour into the mold. Pouring the mixture from an elevated height above the mold will limit the amount of large bubbles or defect in the casting. As in the optimal gripper finger casting, vacuum degassing can also be used to extract air trapped in the mixture. Allow for a minimum of 4 hours of curing time before removing (a 12 hour overnight cure was used in this study). After the mold has been cast, use any remaining mixture or prepare another small batch

and cast a cylinder of approximately 30mm diameter and 25 mm height. Insert another nail or equivalent in the center of the cast. Molding the cylinder can be done with spare polyester film material rolled into a cylinder and taped at the seams. After both casts have had time to cure remove the cast from the mold. Prepare a sheet of cotton that is the approximate size of the top cast. Prepare a small batch of Eco-Flex 00-10 and spread a thin layer in an "X" pattern onto the cotton sheet.

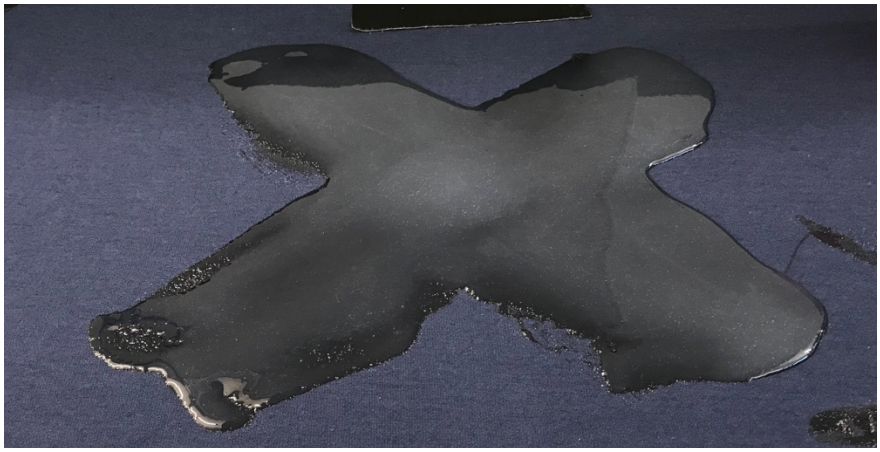

Figure 37. Eco-flex 00-10 spread on cotton sheet.

Place the top mold in the center of the "X". Ensure that the layer of Eco-flex on the cotton layer is not too thick or it will block the pneumatic channels on the top layer and can lead to asymmetric gripper contractions.

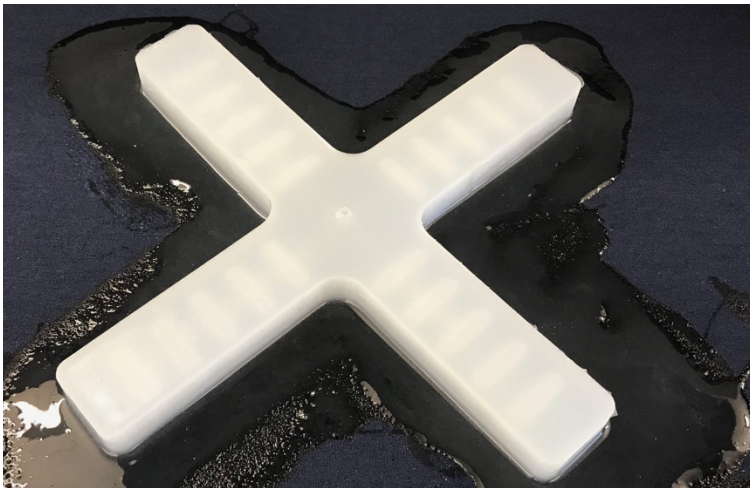

Figure 38. PneuNets top cast curing to cotton layer.

While the top and bottom PneuNet layers are curing, the cylinder can be adhered to the top of the mold. Brush a thin layer of mixed Eco-flex 00-10 on to both surfaces and align tube holes. Once fully cured, the excess cotton layer can be trimmed and the PVC hose can be inserted. A rubber band or sil-poxy can be added to the hose inlet if air escapes during inflation of the device.

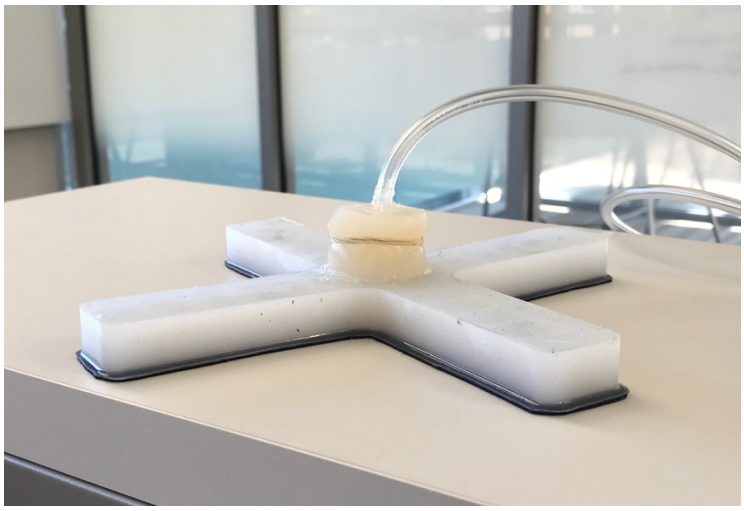

Figure 39. Fabricated PneuNets design.

3.3 Magic-Ball Design

While requiring few steps, folding of the Magic-Ball pattern can be a tedious process. Processing on the Full Spectrum CO_2 laser takes 13 minutes. A power level of 20% and speed of 85% were used to cut the pattern, Figure, into the polyester material. The pattern file was generated in Adobe Illustrator and issues arose when the dotted lines were created. It should be noted that the Full Spectrum software will read dotted lines as solid, unless they are separated in the original Illustrator file. There are many ways to accomplish this, but outlining/expanding the "stroke" of the dotted line will create small rectangular shapes composed of four cuts instead of a single cut. The laser cutter will produce a dotted line, but this will significantly increase the cutting time.

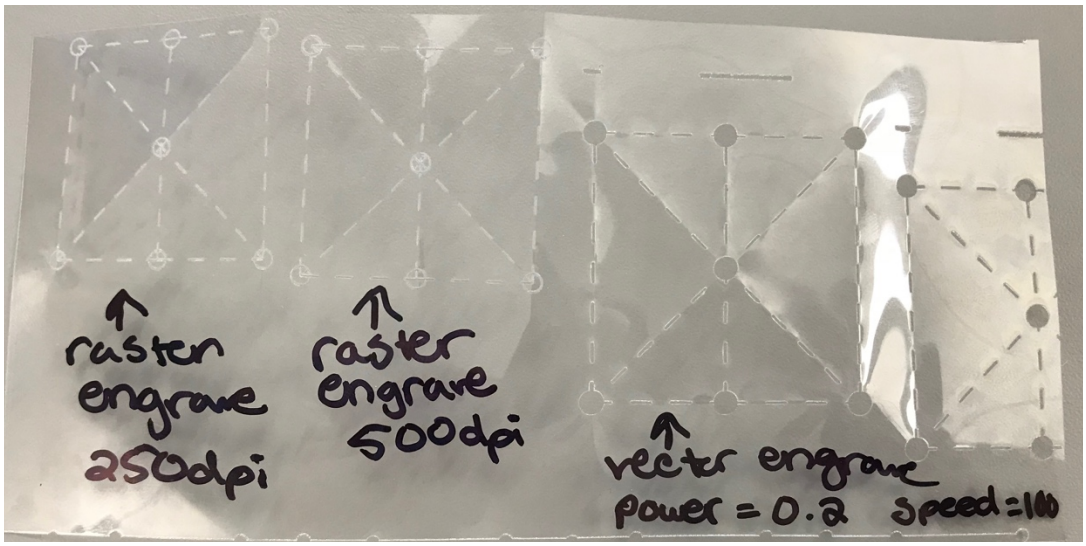

Figure 40. Preliminary testing with different laser settings.

Once the patterned polyester sheet has been folded, the two free ends are taped together with packing tape. Then the "magic-ball" can be formed by re-folding the connected ends and compressing the top and bottom together. A polyurethane film of 0.0015-gauge thickness was used as the skin material. Two circular sheets of approximately 200mm diameter should be cut.

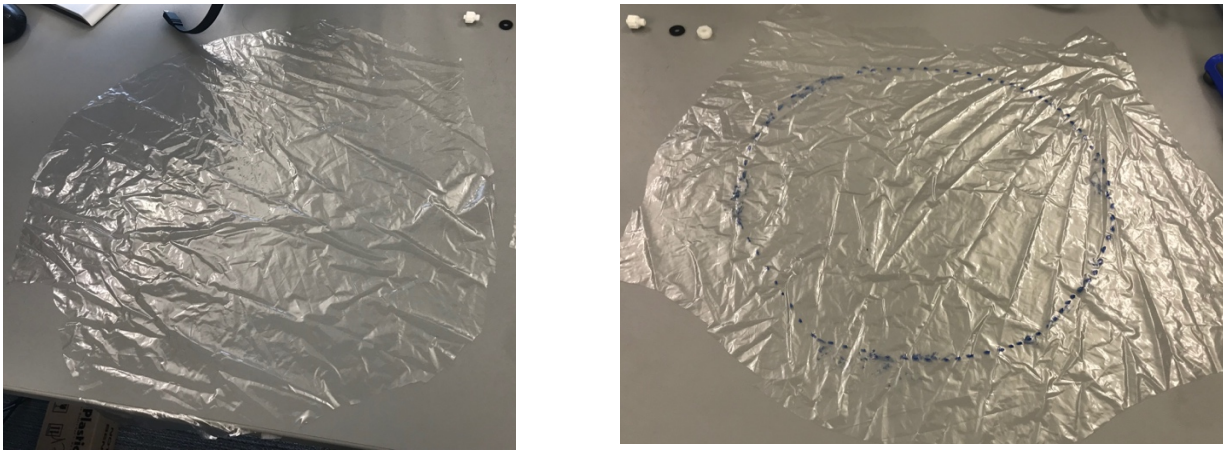

Figure 41. Top polyurethane sheet for magic ball design shown left, bottom sheet with seam trace is shown right

Place one sheet over the top of the “magic-ball” skeleton and the second sheet on into the inner cavity of the skeleton. A 100mm diameter polypropylene sphere was used in this research to keep the inner skin in place while marking the seam locations.

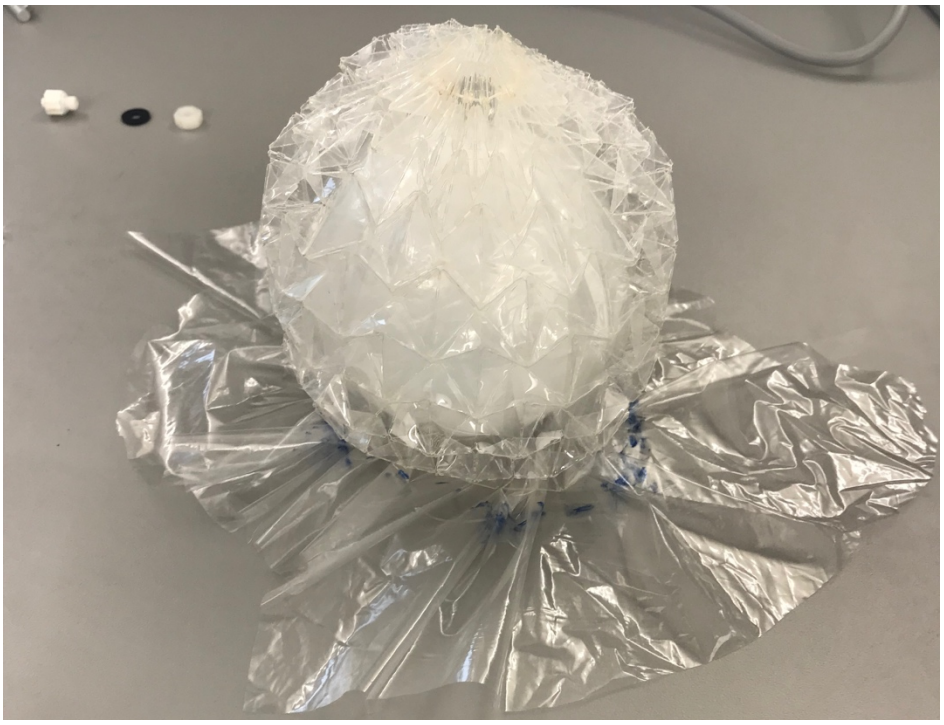

Figure 42. Magic-ball skeleton with sphere holding inner skin in place.

After seams have been marked on both the top and bottom skin, the sphere and skeleton should be removed. Line up the seam lines on both the top and bottom skin and seal on heat setting

number three on the AIE-305 impulse sealer. Leave an opening unsealed and before the skeleton is inserted, install the pneumatic fittings in the center of the top skin. Next, insert the skeleton into the partially sealed skins, and seal the remaining edges.

Figure 43. FOAM magic-ball design.

Chapter 4: Testing Methods

Testing method described in this chapter are a means of evaluating the desirable parameters of an end effector including: grasping strength and variability, grip effectiveness, and performance in a realistic scenario. Very few standardized testing methods currently exist for the end effector designs presented in this work; however, some of the tests are loosely based on similar ASTM testing methods.

4.1 Weighted Grasping Variability

Grasping variability was tested for each end effector design on its ability to securely grasp spherical objects of varying size and varying weights. Four polypropylene spheres of 100mm, 70mm, 50mm, and 25mm diameter were measured at 44, 13, 8, and 2 grams, respectively. Each sphere was incrementally weighted with 50, 100, 200 and 300 grams in addition to the weight of the sphere.

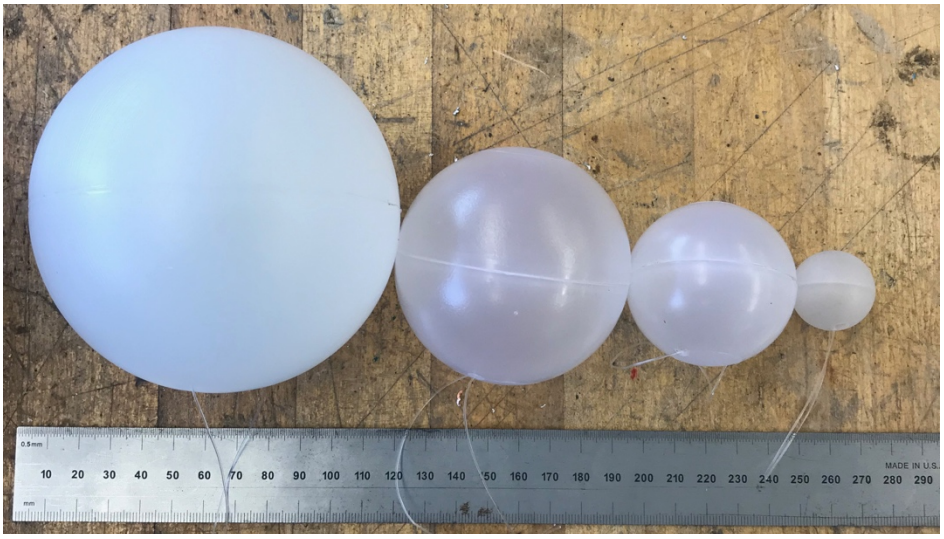

Figure 44. Polypropylene spheres 100, 70, 50 and 25mm diameter with attached monofilament tethers.

A grasping test was considered successful if the end effector could maintain its grip on the sphere for five seconds with out any visible slippage or ejection. If the end effector was able to

successfully grasp each weight increment for a sphere, a maximum weight was attempted by incrementally loading and checking for slippage or ejection until the device failed. All end effectors were positioned in a vertical orientation suspended by monofilament wire. Each sphere was fixed with a length of monofilament wire that could be attached to a paper weight boat, weighing four grams, that was used to hold the weight. Two-inch wood screws, weighing three grams, were used as the mass in this experiment. A 4.7-ounce syringe with two check valves was used as a pump and a vacuum to actuate the designs.

4.2 Grasp Effectiveness

Grasp effectiveness was tested through a series of tests in which an impulse or mechanical shock was induced to the end effector while grasping an object. Each end effector was suspended in a vertical orientation by monofilament wire. A gala apple weighing 140 grams was grasped by the end effector which was then subjected to a series of vertical drops at increments of 5, 10 and 15 centimeters above its starting position. Five trials were performed at each drop interval for every end effector tested. A test was successful if the apple did not slip or eject from the gripper. A secondary test was conducted in which a Bosch BMA280 accelerometer was used to collect acceleration data during test. The device was suspended in a Plexiglas fixture and the end effector was secured below. The testing procedure was identical to the initial impulse test, however, only one trial was completed for each height increment.

4.3 Real World Evaluation

All three end effector designs were tested at an apple orchard at the horticulture farm on Michigan State University's campus. Traditional apple trees that had been trimmed the previous season were selected due to their similarity to possible scenarios found in regenerative farming situations.

Figure 45. Conventional apple orchard tree shown left, compared to "high-density" apple orchard tree shown right.

Each end effector was placed in various scenarios with apples in clusters as well as single apples of varying orientation. The accessibility of the apples was evaluated in this qualitative test for each end effector. An attempt was also made to harvest an apple from the tree with each end effector being manually manipulated by an operator.

Harvesting metrics for Spartan apples, a variety of Macintosh, were tested for one hundred samples on Michigan State University's horticulture farm. Detachment force, apple diameter and weight were recorded during the first week in August 2018. A "fish hook" uniaxial force gauge was attached to the apple during harvesting to record force data. The PneuNets design was used to harvest the first 20, with the remaining 80 samples using the "fish hook" and monofilament sling. Weight was recorded using the same "fish hook" gauge. Diameter was determined using a set of digital calipers.

Chapter 5: Results and Discussion

Chapter five presents the results of the tests performed and then provides a discussion on these results. Only two designs were successfully tested, with the Magic-ball design failing to grasp any of the testing materials without the use of a vacuum pump, which was unavailable at the time of testing.

5.1 Grasping Variability Results

Grasping variability test results in Table 2 show that the optimal grippers design had success with a greater size range, but at a lower weight. Contrary to the optimal gripper results, the PneuNets design successfully grasped a maximum weight of approximately 1.2 kilograms for both the 100 and 70 millimeter spheres. Smaller objects proved to be a challenge for the PneuNets design which was unable to grasp any of the weighted scenarios for the 25 millimeter sphere. Grasping for the optimal gripper was more reliant upon side wall contact between the *fingers* and object being grasped, while the PneuNets design applied a caging style of grasping. The difference between these two methods can be seen in Figure.

Figure 46. Grasping scheme for the optimal gripper shown left, with caging scheme of the PneuNets design shown right.

Table 2. Results from the weighted grasping variability test performed on the optimal gripper and PneuNets designs.

	Sphere (mm)	Added weight (g)	Total weight (g)	Result
Optimal Gripper	100	50	95	pass
		100	147	pass
		200	245	pass
		300	345	fail
	70	50	64	pass
		100	113	pass
		200	213	pass
		300	313	fail
	50	50	59	pass
		100	108	pass
		200	208	pass
		300	308	pass
	25	50	52	pass
		100	103	pass
		200	202	fail
		300	302	fail
PneuNets	100	50	94	pass
		100	144	pass
		200	244	pass
		300	344	pass
		1,199	1243	pass
	70	50	63	pass
		100	113	pass
		200	213	pass
		300	313	pass
		1,199	1212	pass
	50	50	58	pass
		100	108	pass
		200	208	pass
		300	308	fail
	25	50	52	fail
		100	102	fail
		200	202	fail
		300	302	fail

PneuNets and optimal gripper designs were successfully tested; however, a loss of actuation occurred over time for all designs. This is due to the permeability of the materials used in each design. Applying a constant positive or negative pressure would prove beneficial and may have led to improved results.

5.2 Grasping Effectiveness

As shown in Table 3, while the optimal gripper design passed the drop test for the five centimeter displacement, failures occurred during the 10 and 15 cm displacements. Even though the apple was not constrained, the PneuNets design succeeded at all displacement drop increments. During each trial, the caging method used by the PneuNets design allowed the apple to shift within the grasp of the device, however, it did not allow for ejection due to the rigidity of the limbs when inflated.

Table 3. Trial results for grasp effectiveness during drop testing.

	Displacement (cm)	Trial	Result
Optimal Gripper	5	1	pass
		2	pass
		3	pass
		4	pass
		5	pass
	10	1	fail
		2	pass
		3	pass
		4	fail
		5	pass
	15	1	fail
		2	fail
		3	fail
		4	pass
		5	fail
PneuNets	5	1	pass
		2	pass
		3	pass
		4	pass
		5	pass
	10	1	pass
		2	pass
		3	pass
		4	pass
		5	pass
	15	1	pass
		2	pass
		3	pass
		4	pass
		5	pass

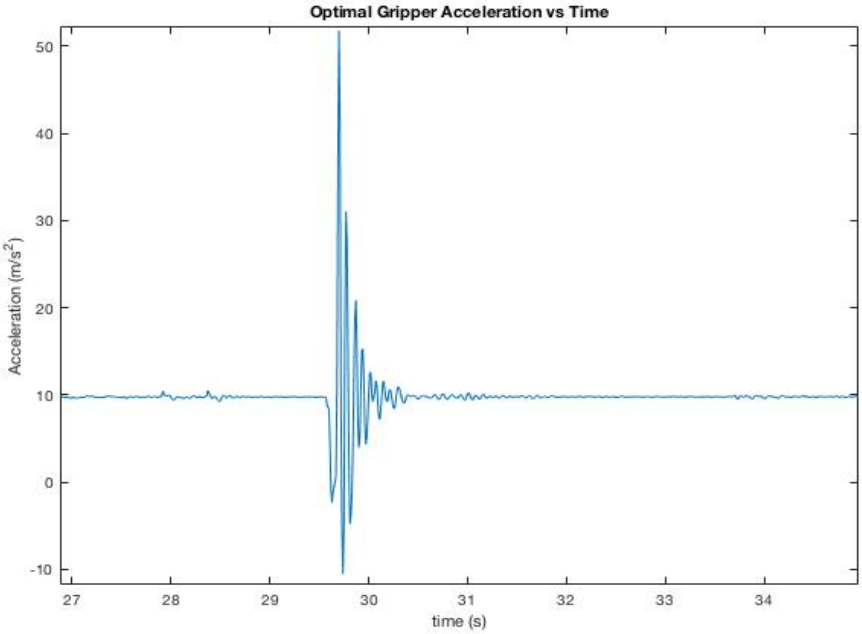

Figure 47. Acceleration graph for 5 cm displacement optimal gripper test.

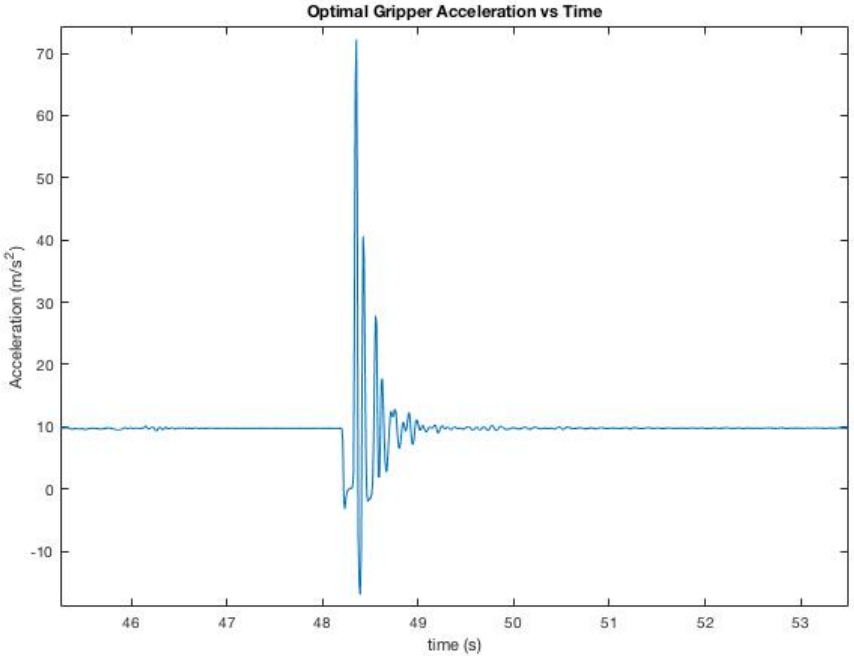

Figure 48. Acceleration graph for 10 cm displacement optimal gripper test.

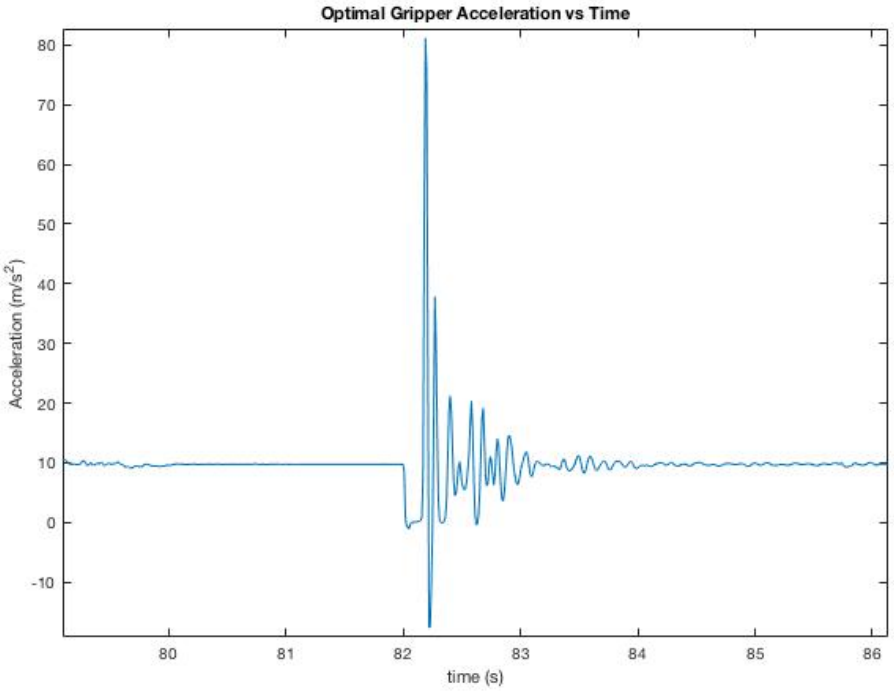

Figure 49. Acceleration graph for 15 cm displacement optimal gripper test.

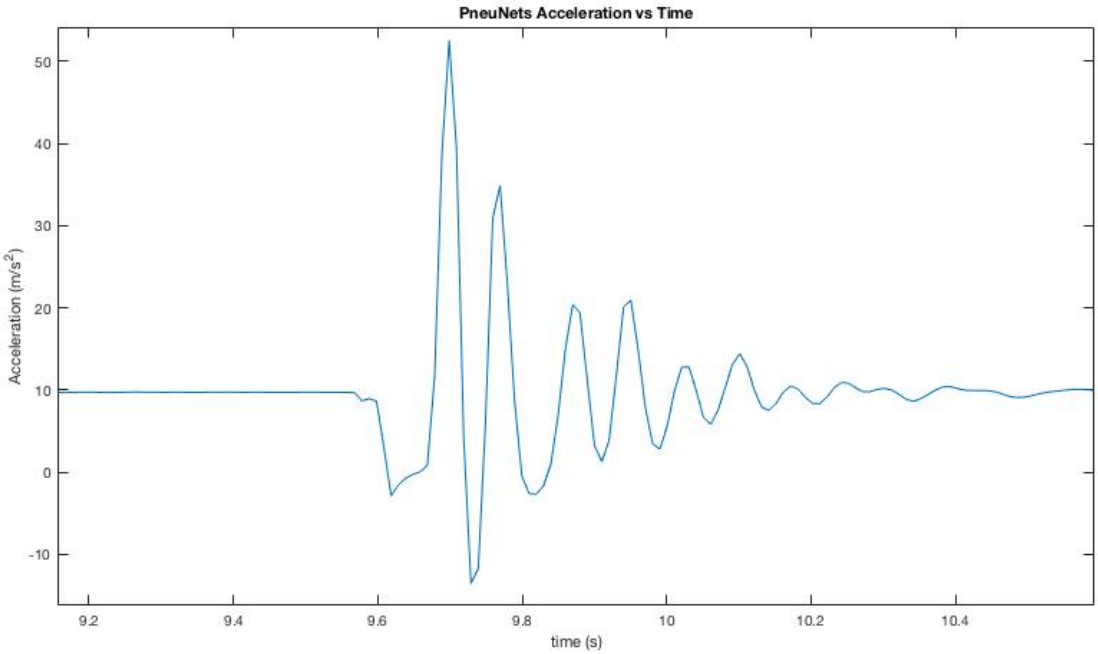

Figure 50. Acceleration graph for 5 cm displacement PneuNets test.

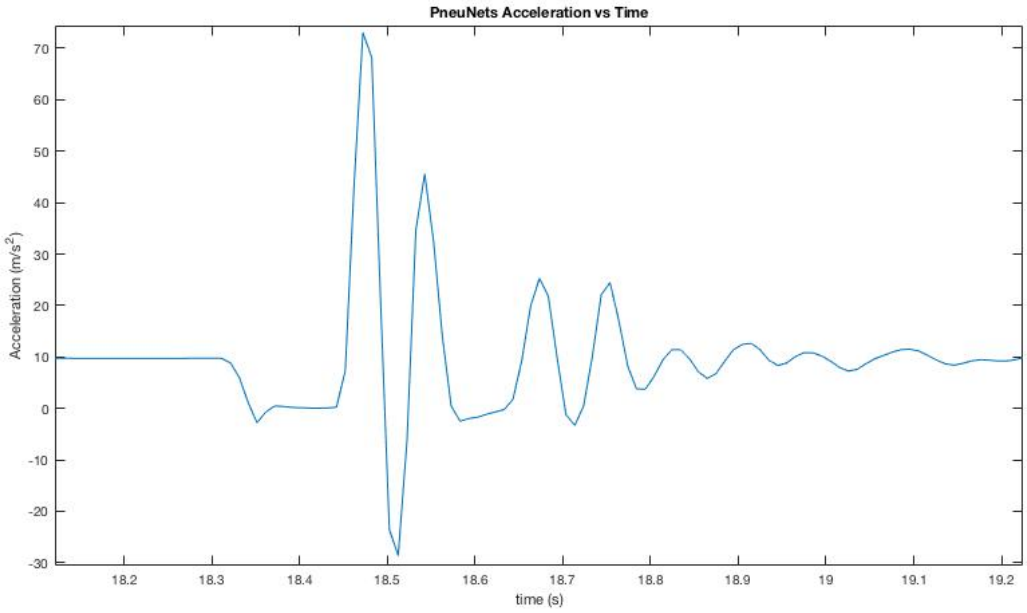

Figure 51. Acceleration graph for 10 cm displacement PneuNets test.

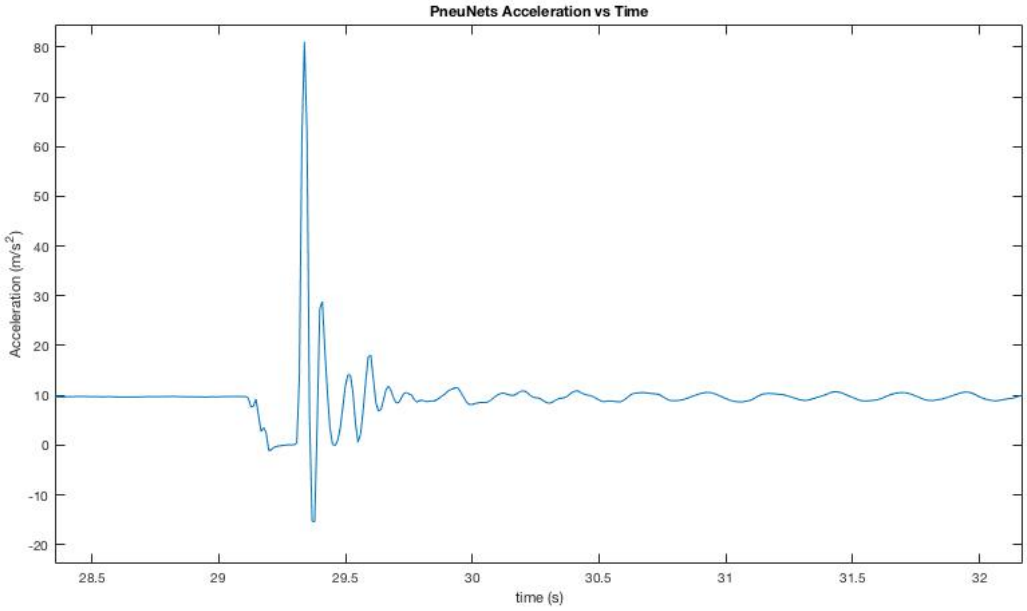

Figure 52. Acceleration graph for 15 cm displacement PneuNets test.

5.3 Real World Evaluation Results

Sampling from the apple orchard evaluation gave insight into the variability in harvesting scenarios that potential end effectors might encounter. While majority of the desirable apples grow on the perimeter of the tree, some desirable apples are covered by branches and foliage creating potential hazards and clearance issues for end effector designs. Apples can be found in both clusters and as individuals in a variety of orientations along the branch. Each growing pattern presents its own unique challenge for approach planning and end effector orientation with relation to the branch.

[A]  [B] 

Figure 53. Apple arrangement on conventionally trimmed orchard trees.

Each end effector was tested on both isolated apples and apples arranged in clusters. When harvesting the isolated apple, the end effector approached the apple from below to avoid accidentally grasping foliage or branches. For the isolated harvesting, the PneuNets design was the only end effector to successfully remove an apple from the branch. During the clustered

harvesting, an angled approach as shown in Figure was taken to avoid interference from the surrounding apples, branches and other foliage. The PneuNets design and the Magic-Ball design both had success removing apples from the branch in the clustered arrangement.

[A]  [B] 

[C] 

Figure 54. End effectors grasping isolated apples from below.

Figure 55. End effectors grasping apples in cluster configuration.

Although apples were successfully harvested by the PneuNets gripper and the Magic-Ball design, the testing done in the orchard was purely for qualitative purposes. No conclusions can be drawn from these samples taken due to a lack of standardization and sample size. With that being said, simulating a realistic grasping scenario gave significant feedback on various elements of each design, including the end effector compliance, dexterity, maneuverability and actuation speed.

Results of the Spartan-Macintosh apple sampling can be seen in Table 4.

Table 4. Results of Apple sampling.

	Average	Standard Deviation
Force (lbf.)	3.15	±1.32
Diameter (mm)	65.23	±4.46
Weight (lb.)	0.24	±0.045

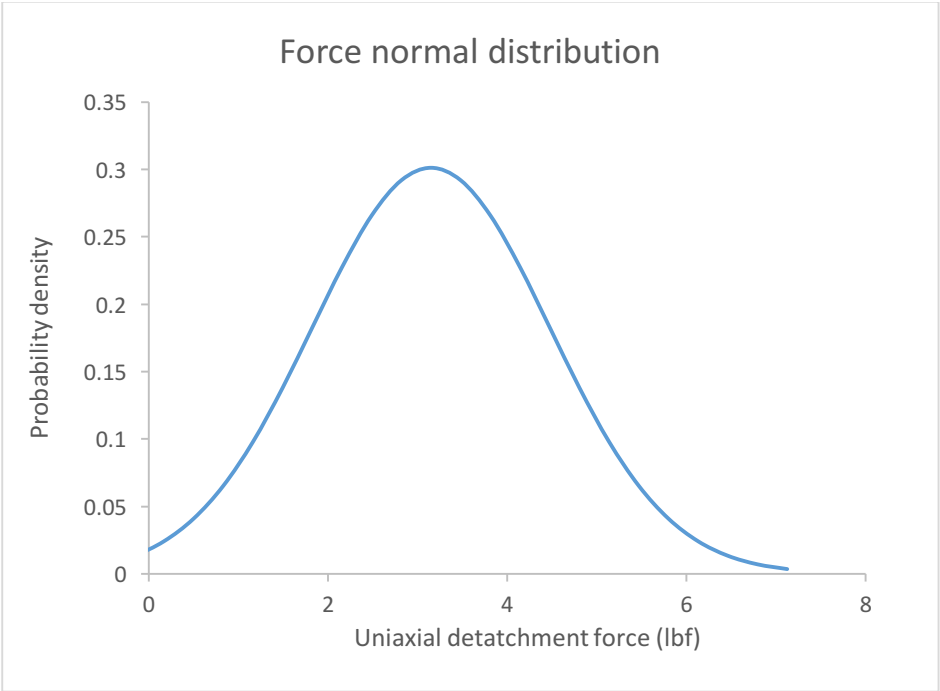

Figure 56. Normal distribution curve for detachment force and probability density of Spartan apples.

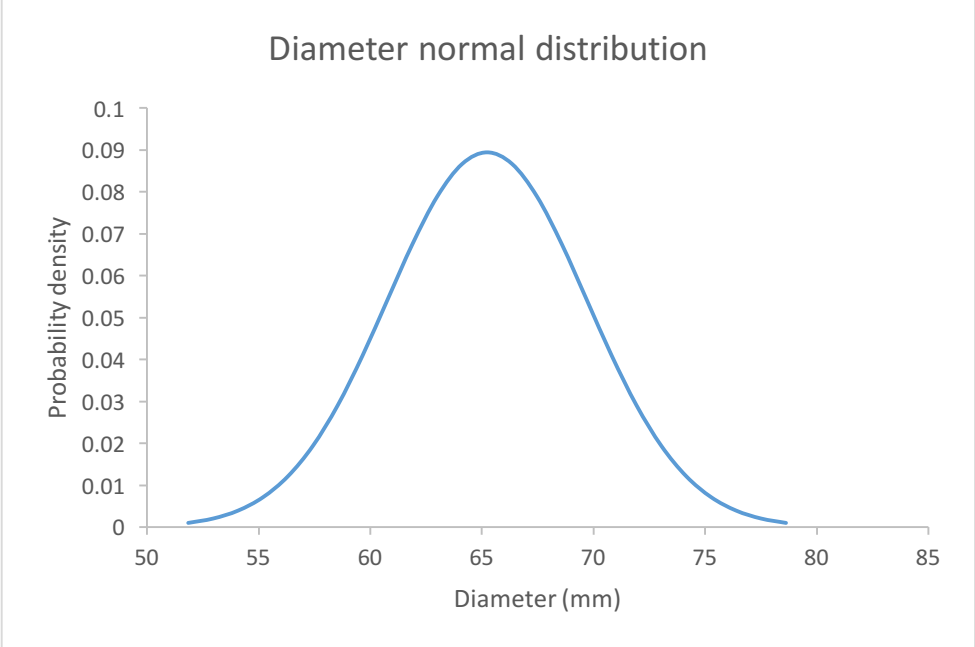

Figure 57. Normal distribution curve for diameter and probability density of Spartan apples.

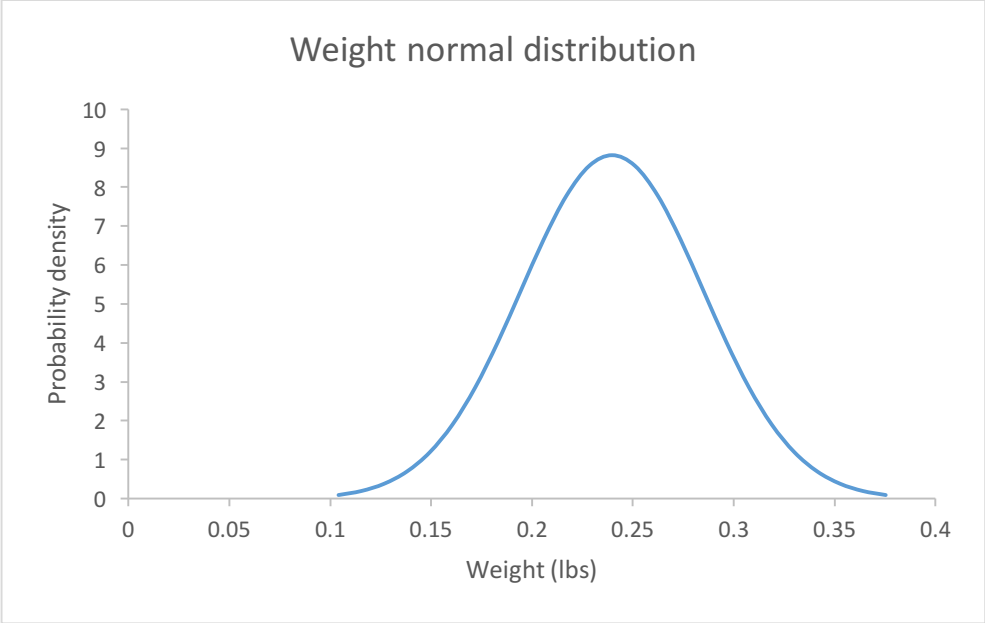

Figure 58. Normal distribution curve for weight and probability density of Spartan apples.

Because these apples were harvested prematurely (not fully ripened), their detachment force might not be exact representations of the forces seen during conventional harvesting periods. The uniaxial pulling harvesting method was the simplest mechanically, but also produced the highest detachment force. Li et al. [39] demonstrated the mechanics of a rotated pulling technique that produces a moment on the stem and lessens the grasping force required to detach the apple.

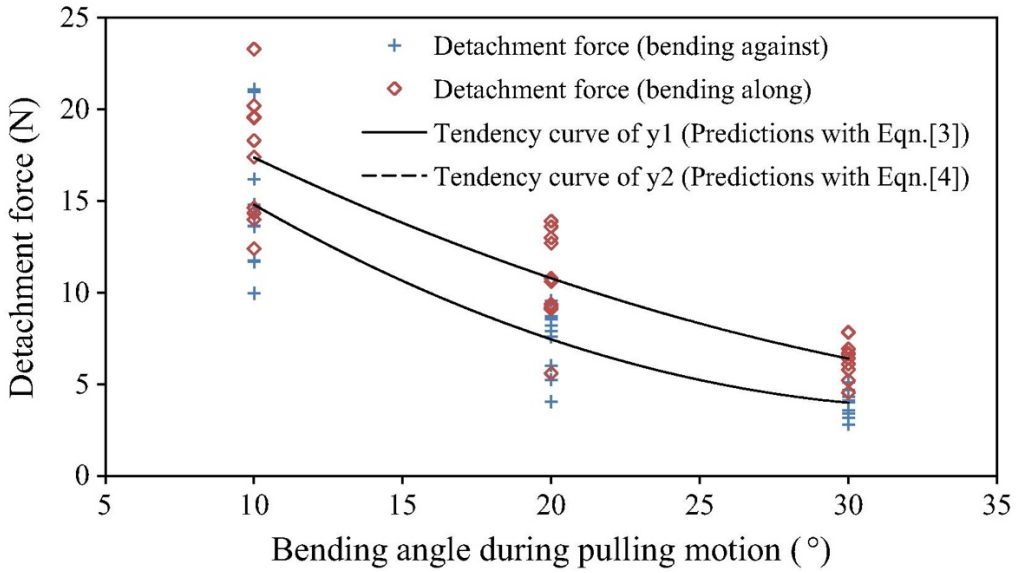

Figure 59. Detachment force versus bending angle during apple harvesting.

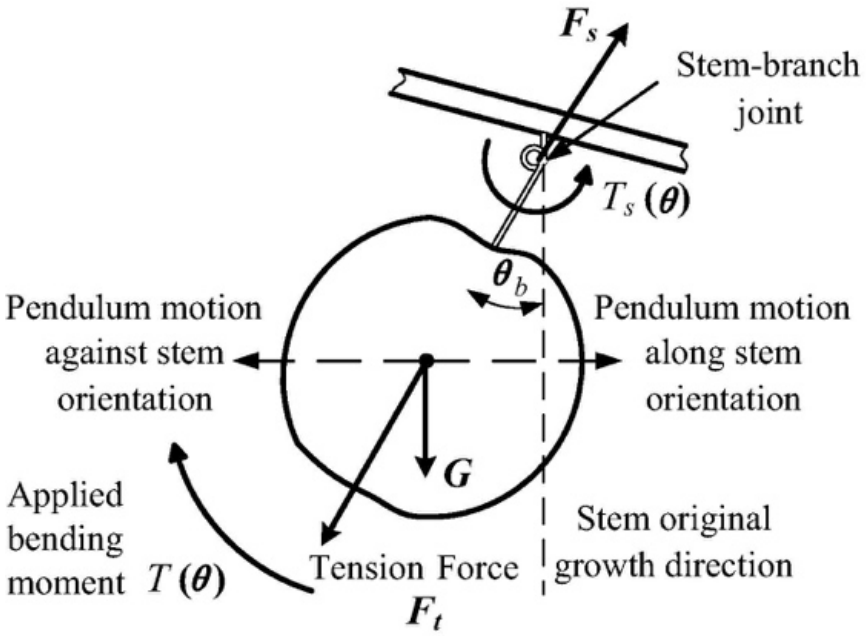

Figure 60. Free body diagram of apple detachment method proposed by Li et al. [39].

Despite difference in detachment technique, the early harvest sample data collected for this study shows similar detachment force values for low angle detachments seen in the work by Li et al. [39].

Chapter 6: Conclusion and Future Work

6.1 Conclusion

Experts are increasingly concerned about the potential for a crisis involving the industrial agricultural complex. Non-regenerative farming practices continue to degrade soil quality and the surrounding environment. Automation through soft robotic presents a novel, low cost and energy efficient method of harvesting produce grown in nonconventional arrangements. The under-actuated end effectors tested in this thesis have shown promising results, and further evaluation should be conducted. Although the majority of the tests conducted were done so in a non-standard qualitative manner, some conclusions can still be drawn about the selection of end effectors. With the particular designs, manufacturing approaches and testing protocols in the current study, the PneuNets and the Optimal gripper designs were the two most successful end effectors, with the PneuNets performing the best overall. At a low cost of $15.59, the simplest manufacturing procedure, a high grasping strength and effectiveness, the PneuNets design shows promise as a viable option for future implementation.

6.2 Future work

A significant amount of future work is required before soft robotics can out-perform human operators in harvesting produce.

Although minimal success was found with the Magic-Ball design, the base technology, FOAM, presents a novel and low cost actuator that can be arranged in a variety of end effector configurations. The potential of utilizing a purely FOAM design should by no means be discounted based purely on the results of this research. When grasping non-spherical objects such as bottles or objects with non-smooth edges, the Magic-Ball design is able to lift significant

weight. Combining the FOAM method with a softer skeleton or adding soft material to the grasping surface of a FOAM design could potentially improve slippage and ejection issues.

Improvements to the optimal gripper design should focus on the stiffness and the shape of the gripper *fingers*. The lack of rigidity in the finger tips led to slippage and ejection with objects of larger mass. Using a material with a larger modulus of elasticity such as flexible filament would also benefit the manufacturing process by removing the need for silicone casting. Having the bulk of the design 3D printed would improve manufacturing time and reduce cost.

For the PneuNets design, changes should be explored that would enhance actuation speed, reduce weight, and decrease pre-actuated foot print. Groups such as Soft Robotics Inc. have been working towards this goal with their pick and place system as seen in Figure. Shifting to the Fast PneuNets design would possibly provide benefits in actuation speed, but the device would be sacrificing some compliance.

This introductory evaluation has shown the possible application for soft robotics in small scale agriculture. While these designs are not optimized, they show potential while remaining significantly less expensive than their conventional counterparts. Future end effector designs should have compliance, speed and produce security as high priority design parameters. Produce damage is also an important factor, which was not directly considered here. Next steps should also include the development of a low-cost robotic limb and vision system to further develop a fully automated harvesting solution for regenerative farms.

BIBLOGRAPHY

BIBLIOGRAPHY

[1] FAO, "High Level Expert Fourm - How to Feed the World in 2050," in *Global Agriculture Towards 2050*, Rome, 2009.

[2] HLPE, "Investing in smallholder agriculture for food security. A report by the High Level Panel of Experts on Food Security and Nutrition of the Committee on World Food Security," Rome, 2013.

[3] J. M. O. Sandra L. Colby, "Projections of the Size and Composition of the U.S. Population: 2014 to 2060," U.S. CENSUS BUREAU, 2015.

[4] The World Bank, "Urban Population (% of total)".

[5] The Department of Economic and Social Affairs of the United Nations, "World Urbanization Prospects The 2014 Revision," New York, 2014.

[6] USDA, "ers.usda.gov," 2016. [Online]. Available: https://www.ers.usda.gov/webdocs/charts/84911/sept17_datafeature_cromartie_fig05.png?v=42976. [Accessed 2018].

[7] A. M.-B. Christopher Barrington-Leigh, "A century of sprawl in the United States," 2015.

[8] Natural Resource Conservation Service, "2007 National Resources Inventory," 2010.

[9] J. Rockstrom, P. Kaumbutho, J. Mwalley, A. Nzabi, M. Temesgen, L. Mawenya, J. Barron, J. Mutua and s. Damgaard-Larsen, "Conservation farming strategies in East and Southern Africa: Yields and rain water productivity from on-farm action research," *Soil & Tillage Research,* vol. 103, no. 2009, pp. 23-32, 2009.

[10] D. A. Sumner, "American Farms Keep Growing: Size, Productivity, and Policy," *Journal of Economic Perspectives,* vol. 28, no. 1, pp. 147-166, 2014.

[11] United States Department of Agriculture, "United States Summary and State Data," 2012.

[12] World Commission on Environment and Development, "Our Common Future".

[13] K. A. Dahlberg, "Sustainable Agriculture: Fad or Harbinger?," *BioScience,* vol. 41, no. 5, pp. 337-340, May 1991.

[14] M. V. Gold, "Organic Production/Organic Food: Information Access Tools," April 2016. [Online]. Available: https://www.nal.usda.gov/afsic/organic-productionorganic-food-information-access-tools. [Accessed July 2018].

[15] K. A. Dahlberg, "REGENERATIVE FOOD SYSTEMS," in *MANAGEMENT OF AGRICULTURAL, FORESTRY AND FISHERIES ENTERPRISES - Vol. II*, MI: Encyclopedia of Life Support Systems.

[16] M. A. Altieri and S. B. Hecht, "Small-Scale Agriculture in SouthEast Asia," in *Agroecology and Small Farm Development*, CRC, 1990.

[17] The Carbon Underground, "What is Regenerative Agriculture?," 24 Feburary 2017. [Online]. Available: https://thecarbonunderground.org/wp-content/uploads/2017/02/Regen-Ag-Definition-7.27.17-1.pdf. [Accessed 2018].

[18] P. Stephen G. Bronars, "A Vanishing Breed How the Decline in U.S. Farm Laborers Over the Last Decade Has Hurt the U.S. Economy and Slowed Production on American Farms," 2015.

[19] S. Bronars, "NO LONGER HOME GROWN: How Labor Shortages are Increasing America's Reliance on Imported Fresh Produce and Slowing U.S. Economic Growth," Partnership for a New American Economy, 2014.

[20] R. STROCHLIC, C. WIRTH, A. FERNANDEZ BESADA and C. GETZ, "FARM LABOR CONDITIONS ON ORGANIC FARMS IN CALIFORNIA," 2008.

[21] S. M. GABBARD and J. M. PERLOFF, "The Effects of Pay and Work Conditions on Farmworker Retention," *INDUSTRIAL RELATIONS,* vol. 36, no. 4, 1997.

[22] Destaco, "End Effectors," [Online]. Available: https://www.destaco.com/end-effectors.html.

[23] A. Robinson, "The History of Robotics in Manufacturing," cerasis, 2014.

[24] UC Davis , "Biological and Agricultural Engineering," [Online]. Available: https://bae.engineering.ucdavis.edu/blog/stavros-vougioukas-awarded-funding-develop-robots-harvest/. [Accessed 2018].

[25] R. Lu, Z. Zhang and A. K. Pothula, "Innovative Technology for Apple Harvest and In-eld Sorting," *NEW YORK STATE HORTICULTURAL SOCIETY,* vol. 25, no. 2, 2017.

[26] D. Bulanon and T. Kataoka, "A Fruit Detection System and an End Effector for Robotic Harvesting of Fuji Apples," *Agricultural Engineering International,* vol. XII, no. 2010, 2010.

[27] J. Davidson and A. Silwal, "Robotic Apple Harvesting in Washington State," in *IEEE Agricultural Robotics & Automation Webinar*.

[28] J. H. TIBBETTS, "Not Too Far From the Tree," 2018. [Online]. Available: https://www.asme.org/wwwasmeorg/media/ResourceFiles/EngineeringTopics/Robotics/0218_ME_CoverStory.pdf. [Accessed 2018].

[29] B. Mosadegh, P. Polygerinos, C. Keplinger, S. Wennstedt, R. F. Shepherd, U. Gupta, J. Shim, K. Bertoldi, C. J. Walsh and a. G. M. Whitesides, "Pneumatic Networks for Soft Robotics That Actuate Rapidly," *Advanced Functional Materials,* vol. 24, no. 15, p. 2163–2170, 2014.

[30] J. Rossiter and H. Hauser, "Soft Robotics - The Next Industrial Revolution? [Industrial Activities]," *IEEE Robotics & Automation Magazine,* vol. 23, no. 3, pp. 17-20, September 2016.

[31] A. Miriyev, G. Caires and H. Lipson, "Functional properties of silicone/ethanol soft-actuator composites," *Materials & Design,* vol. 145, pp. 232-242, May 2018.

[32] Super Releaser, "superreleaser.com/," [Online]. Available: https://superreleaser.com/blog/2017/5/11/a-short-history-of-soft-grippers.

[33] F. Ilievski, A. D. Mazzeo, R. F. Shepherd, X. Chen and G. M. Whitesides, "Soft Robotics for Chemists," *Angewandte Chemie,* January 2011.

[34] S. Li, D. M. Vogt, D. Rus and R. J. Wood, "Fluid-driven, origami-inspired artificial muscles," *Proceedings of the National Academy of Sciences of the United of America,* vol. 114, no. 50, pp. 13132 - 13137, 27 November 2017.

[35] T.-L. C. C.-H. C. M.-C. H. Chih-Hsing Liu, Y. Chen, T.-Y. Pai, W.-G. Peng and Y.-P. Chiang, "Optimal Design of a Soft Robotic Gripper for Grasping Unknown Objects," *SOFT ROBOTICS,* vol. 00, no. 00, 2018.

[36] J. Falco, K. Van Wyk, S. Liu and S. Carpin, "Grasping the Performance Facilitating Replicable Performance Measures via Benchmarking and Standardized Methodologies," *IEEE ROBOTICS & AUTOMATION MAGAZINE,* 2015.

[37] J. Zhang, A. Jackson, N. Mentzer and R. Kramer, "A Modular, Reconfigurable Mold for a Soft Robotic Gripper Design Activity," *Front. Robot. AI,,* september 2017.

[38] Soft Robotics Inc, "Core Technology," Soft Robotics INC, 2018. [Online]. Available: https://www.softroboticsinc.com/core-technology. [Accessed 2018].

[39] J. Li, M. Karkee, Q. Zhang, K. Xiao and T. Feng, "Characterizing apple picking patterns for robotic harvesting," *Computers and Electronics in Agriculture,* vol. 127, pp. 633-640, september 2016.